INTERNATIONAL JOURNAL OF CLIMATOLOGY
Int. J. Climatol. **20**: 19–46 (2000)

ENSO SIGNALS IN EAST AFRICAN RAINFALL SEASONS

MATAYO INDEJE, FREDRICK H.M. SEMAZZI* and LABAN J. OGALLO
Department of Marine, Earth and Atmospheric Sciences, North Carolina State University, Raleigh, NC, USA
Department of Meteorology, University of Nairobi, Nairobi, Kenya

Received 3 April 1998
Revised 31 March 1999
Accepted 6 April 1999

ABSTRACT

The evolutions of ENSO modes in the seasonal rainfall patterns over East Africa are examined in this study. The study covers the period 1961–1990. Both rotated empirical orthogonal function (EOF) and simple correlation analyses were used to delineate a network of 136 stations over East Africa into homogeneous rainfall regions in order to derive rainfall indices. Time series generated from the delineated regions were later used in the rainfall/ENSO analyses. Such analyses involved the development of composite rainfall map patterns for El Niño and post-ENSO ($+1$) years in order to investigate the associations between seasonal evolution of El Niño–Southern Oscillation (ENSO) signals and the space-time evolution of rainfall anomalies over the region.

Analyses based on both EOF and simple correlation techniques yielded eight homogeneous rainfall regions over East Africa. The results showed unique seasonal evolution patterns in rainfall during the different phases of the ENSO cycles. East African rainfall performance characteristics were stratified to identify distinct rainfall anomaly patterns associated with ENSO and post-ENSO ($+1$) years. These can be applied in conjunction with skilful long lead (up to 12 months) ENSO prediction to provide guidance on likely patterns of seasonal rainfall anomalies over the region. Such information can be crucial for early warning of socio-economic disasters associated with extreme rainfall anomalies over East Africa. Copyright © 2000 Royal Meteorological Society.

KEY WORDS: Eastern Africa; empirical orthogonal function; ENSO; rainfall anomalies; seasonality

1. INTRODUCTION

Rainfall is the climatic factor of maximum significance for the East African countries, with extreme occurrences resulting in droughts and floods, which are often associated with food, energy and water shortages, loss of life and property, and many other socio-economic disruptions. The economies of East African countries largely depend on agriculture, which is highly vulnerable to the amounts and distribution of rainfall. The efforts to achieve food security in most parts of the African continent including East Africa have long been hampered by civil wars, political volatility, worsening conditions of international trade, rapid population growth, floods and drought. Floods and droughts are natural events, which cannot be controlled. However, in East Africa, like some other parts of the world including India and South Africa (Dyer, 1981), there are prospects for out-of-season rainfall compensation of the deficit conditions. Accurate seasonal to inter-annual climate monitoring and forecasting could therefore contribute to improved planning and the management of climate sensitive activities, involving agricultural and water resources, hydroelectric power supply and tourism, among others. There are other factors such as fires, spread of diseases etc., which are linked to climate variability, some of which have been discussed by Glantz (1974).

Several attempts have been made to study the spatial and temporal variability of rainfall in East Africa (Rodhe and Virji, 1976; Ogallo, 1983, 1988; Barring, 1988; Beltrando, 1990; Nyenzi, 1990; Nicholson, 1996). Rodhe and Virji (1976) analysed the trends and periodicity for annual rainfall over East Africa.

* Correspondence to: North Carolina State University, Department of Marine, Earth, and Atmospheric Sciences, Raleigh, NC 27607-8208, USA.

CCC 0899–8418/2000/010019–28$17.50

Spectral analysis of the time series revealed major peaks centred on 2–2.5, 3.5 and 5.6 years. Ogallo (1980) and Ogallo *et al.* (1994) have shown the existence of three major peaks, centred on the Quasi-Biennial Oscillation (QBO) of 2.5–3.7 years, El Niño–Southern Oscillation (ENSO) of 4.8–6 years and the sunspot cycle of 10–12.5 years. Nicholson and Nyenzi (1990) and Nicholson (1996) observed a strong quasi-periodic fluctuation in the East African with a time scale of 5–6 years corresponding to the ENSO and sea surface temperature (SST) fluctuations in the equatorial Indian and Atlantic Oceans.

Several studies have used principal component analysis techniques to examine the temporal and spatial variability of rainfall in East Africa (Atwoki, 1975; Ogallo, 1980, 1983, 1988, 1989; Barring, 1988; Nyenzi, 1990; Semazzi *et al.*, 1996). Ogallo (1989) investigated rainfall variability using the rotated principal component analysis (RPCA) method, to characterize the seasonal rainfall over East Africa for the period 1922–1983. The results showed seasonal shifts in the patterns of the dominant RPCA modes that were similar to the seasonal migration of the rainfall patterns associated with the Inter-tropical Convergence Zone (ITCZ). The first two eigenvectors, which generally represent the dominant wet and dry episodes, accounted for a maximum of 58% of the variance. Recent singular value decomposition (SVD) work by Semazzi and Indeje (1999) has identified the bipolar nature of rainfall over southern and eastern Africa. There is at least the implication of a pattern with wave-like features that travel northwards from southern Africa to eastern Africa and the migration of the ENSO-related rainfall anomalies across the entire continent of Africa during the annual cycle.

The ENSO phenomena is known to be a fundamental and quasi-periodic feature of the ocean-atmosphere system, with periodicities ranging from seasonal to about 8 years (Rasmusson and Carpenter, 1983; Halpert and Ropelewski, 1992). Some extreme rainfall anomalies in East Africa have been associated with ENSO (Ropelewski and Halpert, 1987; Janowiak, 1988; Ogallo, 1988, among others). Ropelewski and Halpert (1987) in their study of the relationship between global rainfall and the Southern Oscillation Index (SOI), concluded that, although the statistical association between rainfall over East Africa and the SOI was weak, there was a high probability of abnormally wet conditions in the region during El Niño years. The 1997–1998 ENSO event associated with catastrophic disruption of socio-economic infrastructure and loss of life in East Africa appears to give further support to this notion. Ogallo (1988) observed significant teleconnections between the SOI and seasonal rainfall over parts of East Africa, especially during the northern hemisphere autumn and summer seasons, with the strongest relationships being observed along the Kenyan coast in autumn. Janowiak (1988) showed evidence of association between rainfall anomalies during the austral summer over eastern and southeastern Africa and both the warm (El Niño) and cold (La Niña) phases of ENSO events. The high skill in predicting ENSO phases up to a year in advance (Cane *et al.*, 1986) suggests high prospects of successful applications of ENSO forecasts to seasonal climate prediction in East Africa. ENSO explains about 50% of the East African rainfall variance (Ogallo, 1988), with other factors explaining the remaining variance. Sustainable development in East Africa could benefit significantly from these recent advances in the prediction of short-term climate variability.

A considerable amount of research work has been done in the East African region to explore rainfall/ENSO relationships. Relatively less attention has been directed to the investigation of the effects of ENSO on rainfall in different sub-regions of East Africa. The objective of this study is to identify for the sub-regions of East Africa aspects of rainfall variability which are associated with ENSO. First, we perform cluster analysis on data for the East African rainfall stations network, using both the EOF and simple correlation analysis to identify homogeneous regions of climate variability. Then we investigate the teleconnections between East African seasonal rainfall and ENSO to find seasons and regions that are wet/dry during the El Niño onset and post-ENSO ($+1$) years. The analysis is based on performing composite rainfall map patterns corresponding to the timing of the ENSO onset and post-ENSO ($+1$) years to delineate regions that are wet/dry during these episodes, thus providing geographically detailed information on the climatic risks to be expected when ENSO phenomena occur. The area of study covers three countries (Kenya, Uganda and Tanzania) which are within the drought monitoring project for East, Central and Southern Africa. The region is enclosed by latitudes 5°N–12°S and longitudes 29°E–42°E (Figure 1(a)). The seasonal rainfall patterns in East Africa are controlled by the seasonal migration of the

ITCZ. The complex topographical patterns, the existence of large lakes, variations in vegetation type and land–ocean contrasts give rise to high spatial and temporal variation in precipitation over the region. Other factors known to influence precipitation over East Africa include tropical storms, easterly waves, jet streams, the continental low-level trough, and extra-tropical weather systems (Ogallo, 1989). The data used in this study and methodology are presented in section 2. The results are discussed in section 3 and the conclusions in the section 4.

2. DATA AND METHODS

The data used in this study consist of rainfall records for 136 stations scattered over East Africa (Figure 1(a)). Figure 1(b) shows the delineated homogeneous rainfall regions over East Africa described in the sub-section 3.1. The initial data consist of monthly rainfall totals for the period 1961–1990. The rainfall monthly anomalies were computed by subtracting the monthly climatological means based on the 1961–1990 climatology from the values, and normalized by dividing each record by the corresponding monthly standard deviation. The rainfall data were initially subjected to statistical quality control. Using both the empirical orthogonal function (EOF) analysis method and simple correlation analysis, the 136 rainfall stations were grouped into homogeneous regions. EOF and simple correlation analyses were further used to identify stations most representative of each region. These were then averaged to give a rainfall index representative of each of the delineated regions. Linkages between the observed rainfall anomalies in East Africa and different phases of ENSO were investigated, and seasonal rainfall patterns associated with the various ENSO evolution cycles identified. Analysis of the composite map patterns for monthly and seasonal rainfall for both ENSO onset and post-ENSO (+1) years were based on the

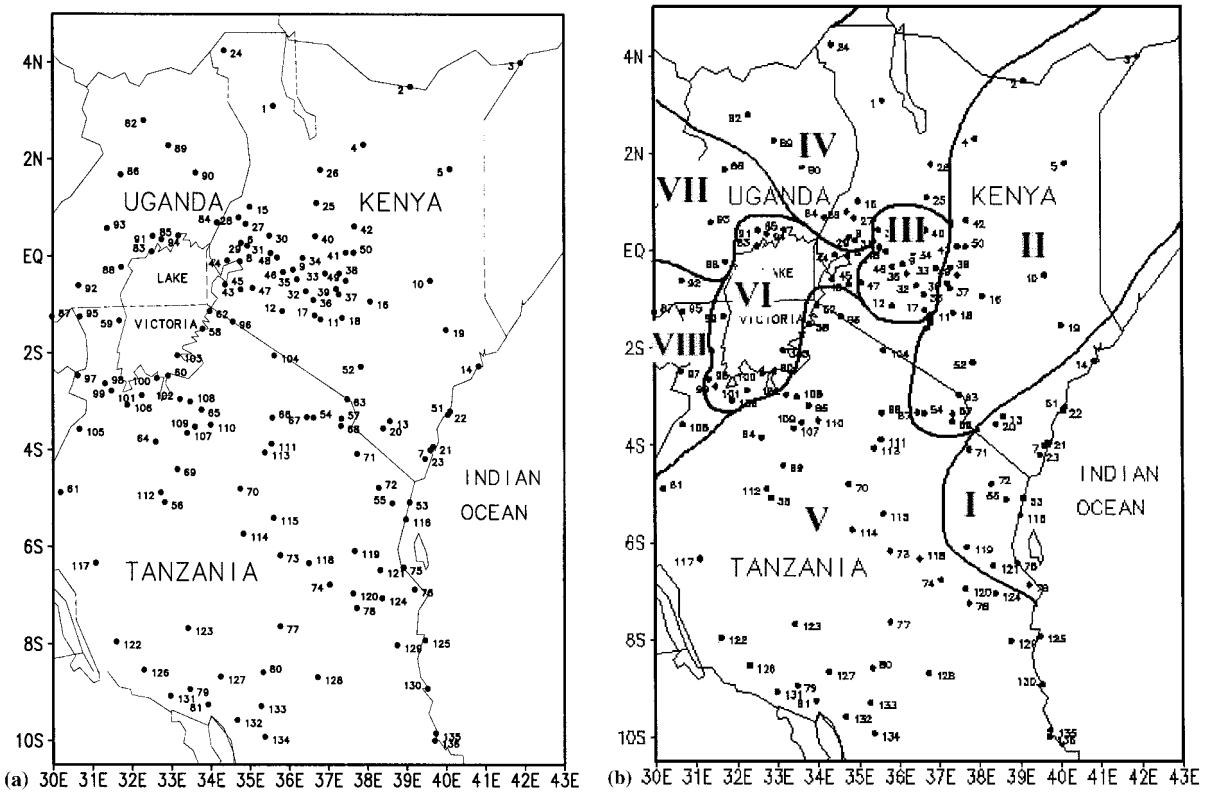

Figure 1. (a) Network of rainfall stations used in this study. (b) The eight homogeneous rainfall grouping over East Africa obtained from combined EOF and simple correlation analyses

delineated homogeneous rainfall regions. Composite rainfall map patterns for ENSO onset and post-ENSO (+ 1) years were generated to delineate regions within East Africa that are wet/dry during these episodes. The November–December–January Niño3 Central Pacific Ocean sea-surface temperature anomaly index was employed to identify the years coinciding/following warm ENSO events during the period 1961–1990. Based on this analysis, warm ENSO events occurred in 1963, 1965, 1968, 1969, 1972, 1976, 1982, 1986, and 1987 (Figure 8). This classification in ENSO years is consistent with those identified earlier (Rasmusson and Carpenter, 1983; Wang, 1984; Nicholson, 1996). The years 1964, 1966, 1970, 1973, 1977, 1983, and 1988 were stratified into the post-ENSO (+ 1) /rainfall composites. The 1982 warm ENSO stands out as the strongest event observed during the period of study. Further analyses were carried out to determine possible shifts in the rainfall seasons in each of the homogeneous rainfall sub-regions of East Africa.

2.1. Spatial clustering of the East African rainfall observations network

Seasonal rainfall patterns over East Africa are very complex due to the existence of complex topography and large inland water bodies. Examples of seasonal rainfall variations for selected regions are shown in Figure 3, for Mubende (central Uganda), Mondo (southwestern Tanzania), Majimazuri (central Kenya) and Mombasa (coastal Kenya). Significant geographical variations have also been observed in ENSO signals over East Africa (Ogallo, 1988), which suggest the need to adopt different empirical models for seasonal climate predictions over different parts of East Africa. Reduction of regional data and delineation of homogeneous regions is therefore necessary for future development of empirical rainfall forecasting models for the region. Regionalization and averaging of rainfall over large but homogeneous regions have the advantages of reducing meteorological noise in the data as well as minimizing the number of variables which describe the regional climate variability. The homogeneous rainfall regions could also be used in the verification of the numerical climate model runs over the East African region (Sun *et al*., 1999a,b). The statistical techniques employed in this study will not only delineate homogeneous rainfall regions over East Africa but will also identify stations most representative of each sub-region.

EOF analysis and simple correlation were used to delineate homogeneous climate regions in East Africa using annual rainfall data. The method used in this analysis is a modified version of the technique employed by Ogallo (1988) and similar to the one adopted by Dyer (1977). EOF analysis enables fields of highly correlated data to be represented adequately by a small number of orthogonal functions and corresponding orthogonal time coefficients, which account for much of the variance in their spatial and temporal variability. Kutzbach (1967) provides a lucid outline of the mathematical procedure necessary to define the functions and their time coefficients. There are a number of examples of applications of EOF analysis to meteorological fields (Tremberth, 1974; Barnett and Davies, 1975; Weare *et al*., 1975; Dyer, 1977; Richman, 1981; Semazzi *et al*., 1996). Rotation of EOF has the effect of redistributing the variance within the eigenvectors and therefore removing the ambiguities while conserving the variance extracted by the selected subset of non-rotated eigenvectors. Various methods of determining the number of significant EOF modes to retain for rotation have been discussed (Kraiser, 1959; Anderson, 1963; North *et al*., 1982; Overland and Preisendorfer, 1982). North *et al*. (1982) have suggested the use of sampling errors in determining the number of significant eigenvectors. The sampling error test is based on comparison of sampling errors for the eigenvalues and the amount of separation from the neighbouring eigenvectors. If the sampling errors in the eigenvalues are comparable to the distance from the nearby eigenvalue, then the sampling errors in the EOF will be comparable to the nearby EOF. In our analysis we adopted the criteria of Kraiser (1959) and North *et al*. (1982) in determining the number of dominant EOF modes to be retained and rotated. Delineation of a homogeneous area was accomplished by identifying the stations with the largest correlation with the principle component (PC) time series associated with the first eigenvector of the annual rainfall anomaly. Each PC time series obtained from EOF analysis was correlated with the stations' rainfall data and areas that correlated significantly exceeding 0.6 correlation coefficient (at 5% level), were identified. These stations were retained and used to delineate the

corresponding region. Stations were then annotated on the map according to the eigenvectors to which they were most strongly related. The procedure was repeated for the remaining stations until all the rainfall stations were assigned to a region. For stations retained through this process in each sub-region EOF analysis was performed again and the important PC time series were correlated with the stations within that region. The stations with correlation coefficients less than 0.6 with the dominant PC were rejected in this iterative process. This procedure was repeated until all the stations in each sub-region had a correlation of 0.6 or more with the first PC at the last iteration. The remaining stations were then averaged to obtain a regionally representative rainfall time series for use in the ENSO/rainfall analysis (section 3.4). This method has proved to be satisfactory with precipitation which is a difficult weather parameter to estimate and should therefore be of value when analysing another parameter like wind (Dyer, 1977).

3. RESULTS

The results obtained from this study are discussed in the following sub-sections. In the sub-section 3.1 we discuss the mean rainfall patterns over East Africa. In the sub-section 3.2, clustering of East African rainfall into homogeneous regions and results obtained from the EOF analysis are discussed. In the sub-sections 3.3. and 3.4, we present the results obtained from the composite rainfall map patterns for ENSO onset and post-ENSO ($+1$) years, and the ENSO modulated seasonal shifts in the regional rainfall, respectively.

3.1. Mean rainfall patterns

Figure 2 shows long-term mean annual rainfall over East Africa based on 1961–1990 climatology. On average more than 800 mm of annual rainfall are observed over areas bordering Lake Victoria to the west, and the Indian ocean to the east. The highlands of central Kenya and southern Tanzania, much of Uganda and western Tanzania also receive rainfall of more than 800 mm, with the northern and eastern parts of Kenya and east central Tanzania, which are semi-arid, receiving less. East Africa exhibits high seasonal rainfall variability ranging from unimodal, bimodal and trimodal rainfall distributions, as shown in Figure 3 which displays some examples of the annual cycle for rainfall over East Africa from four stations in four different homogeneous regions. Four rainfall seasons were chosen for the further analyses; January–February (JF), the 'long rains' of March–May (MAM), June–September (JJAS) and, the 'short rains' of October–December (OND). Figure 4 displays the spatial patterns of the mean seasonal rainfall over East Africa based on the four chosen rainfall seasons. In the JF season, the rainfall is concentrated over the lake regions and most parts of Tanzania. This seasonal rainfall is associated with the extreme southward location of the ITCZ and partly with moisture influx from the Indian ocean. About 42% of the total regional annual rainfall is observed during MAM rainfall season, with the highest intensity observed near the water bodies of the Indian ocean, Lake Victoria and the East African highlands. During this season only weak correlation has been found between rainfall time series at different stations (Ogallo, 1980, 1983; Beltrando, 1990; Nyenzi 1990) because of the large spatial rainfall variability. The high rainfall variability suggests dominance of local factors rather than large-scale factors in the modulation of rainfall patterns during this season. The JJAS rainfall season which accounts for about 15% of the total regional annual rainfall is confined to the western highlands of Kenya, the coastal areas and most parts of Uganda. The OND rainfall season contributes about 25% of the total regional annual rainfall and is well distributed in the whole of East African region. Earlier researchers (Ogallo, 1983; Beltrando, 1990; Nyenzi, 1990; Nicholson, 1996) have found significant station to station correlation and seasonal rainfall to annual rainfall correlations during this season. The dominance of large-scale weather systems may be responsible for the spatial homogeneity of rainfall during this season.

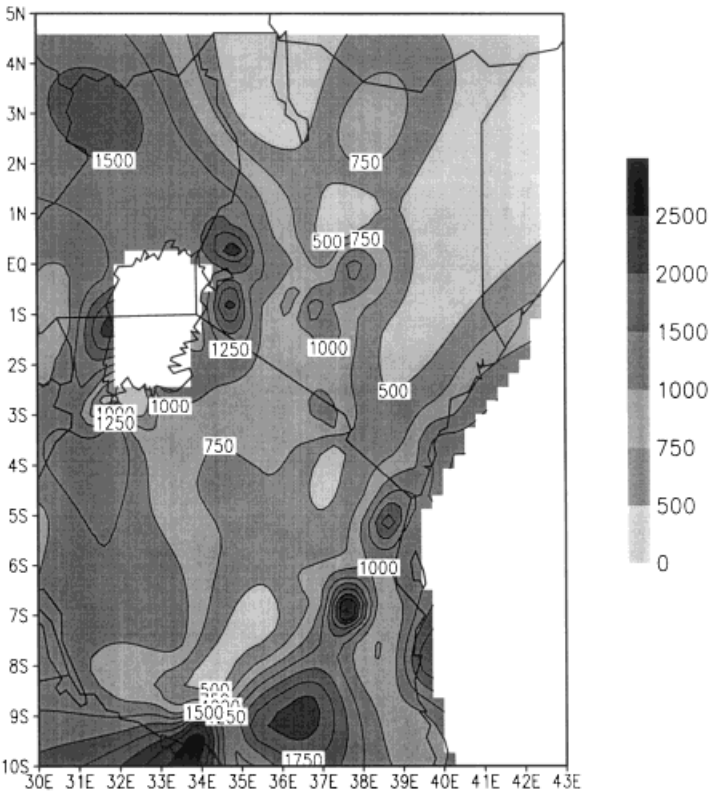

Figure 2. Long-term mean annual climatological rainfall over East Africa (1961–1990). Units are mm

3.2. Clustering East African rainfall stations into homogeneous regions

Based on the criteria used by North *et al.* (1982) a maximum of three EOF modes were found to be distinctly above the noise level for the MAM and OND rainfall seasons. The Monte Carlo significance test described by Overland and Preisendorfer (1982) suggested that two of the three modes are significant at the 5% level. Hence, the third mode may not be statistically significant. However, using Kraiser (1959) sampling techniques, up to four EOF modes had eigenvalues greater than unity and could hence be retained for rotation. The four EOF rainfall modes identified by Kraiser's method explain more that 70% of the total variance and are more representative of the regional seasonal rainfall than the first two modes identified using the North *et al.* criteria. Up to a maximum of 12 modes were above the noise level for the annual rainfall and accounted for more than 75% of the total rainfall variance. Figures 5 and 6 display the contour patterns of the first and second rotated eigenvectors for the seasonal rainfall anomalies for the MAM and OND seasons. Figure 7 shows the corresponding rotated EOF modes for annual rainfall. The spatial patterns of the first component of the rotated EOF modes for the MAM and OND rainfall seasons are shown in Figures 5(a) and 6(a). This pattern accounts for 24.6 and 52.7% of the total variance for the two rainfall seasons respectively. The first EOF mode is in phase throughout the analysis and most of the eigenvector coefficients are negative for the MAM season (Figure 5(a)) and positive for the OND season (Figure 6(a)). The highest values are concentrated over the East African highlands extending to the east to cover the coastal areas of the Indian Ocean. The principal mode (in phase everywhere) is comparable to the flow patterns over the region (Ogallo, 1989). The dominant mode is related to the migration of the ITCZ, which is mainly responsible for seasonal rainfall in the region. The low variance explained by the first EOF mode for the MAM rainfall as compared to that of OND rainfall season, suggests that factors other than global teleconnections play an important role in modulating the ITCZ. The first EOF mode of the OND rainfall season display an east/west dipole pattern with more weight

centred over the East African highlands extending south to cover parts of Tanzania and the East African coast. The spatial pattern of the first EOF rainfall mode is well distributed over the domain and since this mode explains more that 50% of the rainfall variance, confirms the fact that rainfall during this season is spatially well correlated over East Africa. The east/west orientation of the first EOF mode during this rainfall season also suggests that the short rains are more influenced by the east/west oscillating meridional component of the ITCZ. Similarly, the long rains (MAM) are more influenced by the north/south movement of the zonal arm of the ITCZ in the region and other weather systems such as the meso-scale systems, interactions between extra-tropical and tropical weather systems among others (Ogallo, 1989; Beltrando, 1990).

The spatial patterns of the second EOF rainfall components are given in Figures 5(b) and 6(b). They are associated with the intra-seasonal rainfall variability. These patterns account for 10.8 and 6.1% of the rainfall variance for the MAM and OND rainfall seasons, respectively. The MAM coefficients over the eastern parts of the East African highlands and western parts of the Lake Victoria regions, and those of the western parts of the East African highlands, are of opposite signs (Figure 5(b)). This component represents a compensatory system. In those years where the intra-seasonal rainfall exhibits large positive anomalies over the western highlands, below normal rainfall anomalies are observed over the eastern highlands and the western parts of the Lake Victoria basin. The converse is also true since the reference for signs of the coefficients are arbitrary. These conditions may be linked to the intra-seasonal variability of rainfall over the region which is controlled by the interactions between the large-scale easterly flow and the coupling between the Lake Victoria land/lake breeze and the eastern Africa highlands-induced upslope/downslope diurnal mesoscale circulation systems. Both observational studies (Alusa, 1976; Asnani and Kinuthia, 1979) and numerical studies (Okeyo, 1986; Mukabana and Pielke, 1996; Indeje and Anyamba, 1998) have associated the observed afternoon hail and thunderstorm activities over the western parts of the Kenya highlands to the interactions between the prevailing easterly flow and the diurnal meso-scale circulations in the region. The eastern parts of the Kenya highlands and the western parts of the Lake Victoria basin are observed to receive most of the rainfall during the morning hours. The influence of a westerly moist unstable airmass is also responsible for the intense convection over the Kenya highlands (Vincent *et al.*, 1979).

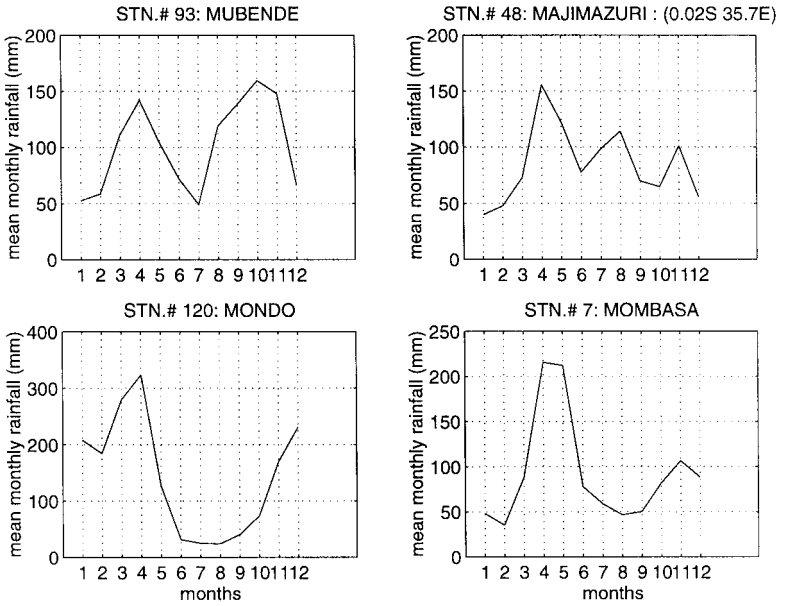

Figure 3. Examples of mean seasonal patterns of rainfall for some selected stations over East Africa

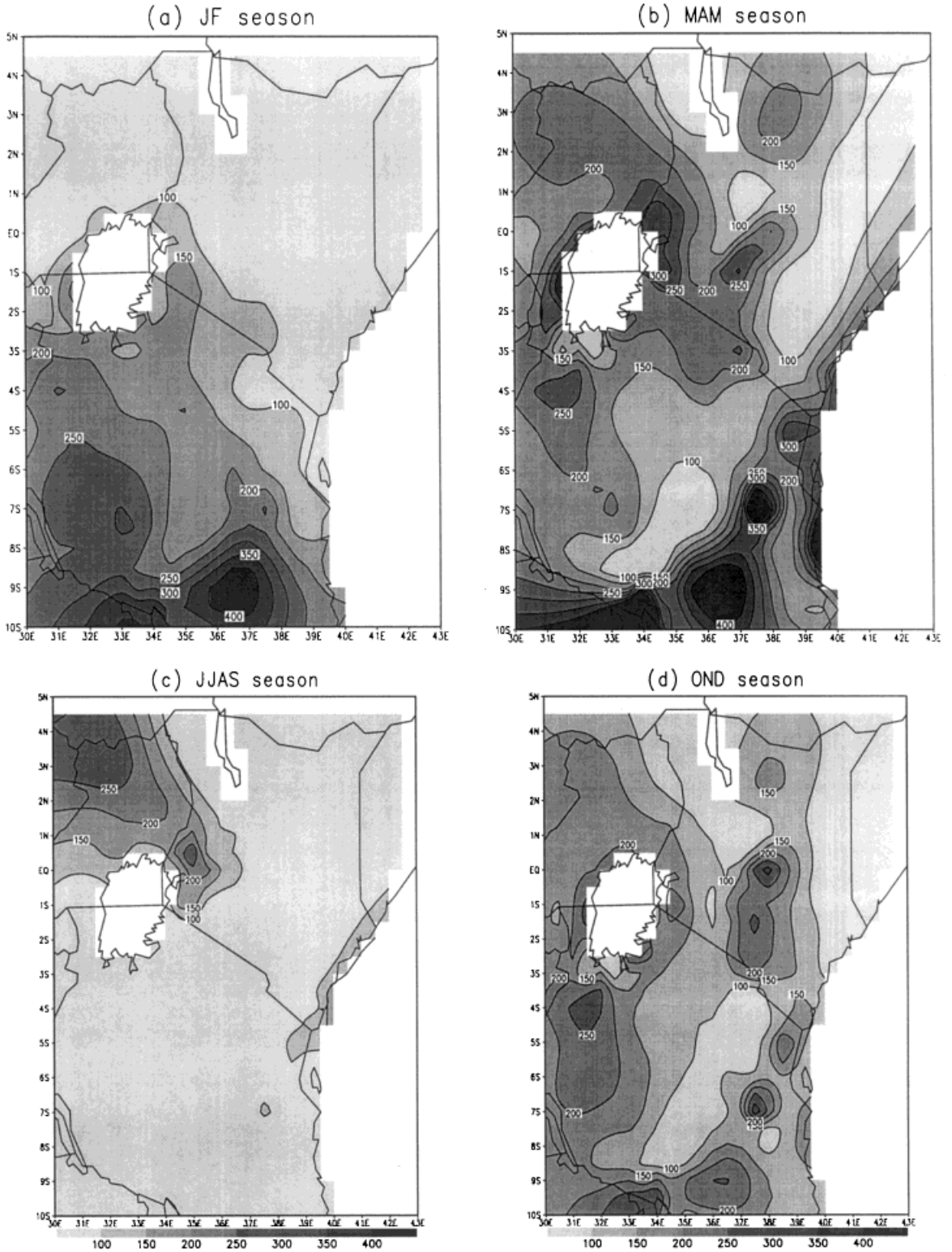

Figure 4. The spatial patterns of the mean seasonal rainfall East Africa. Units are mm

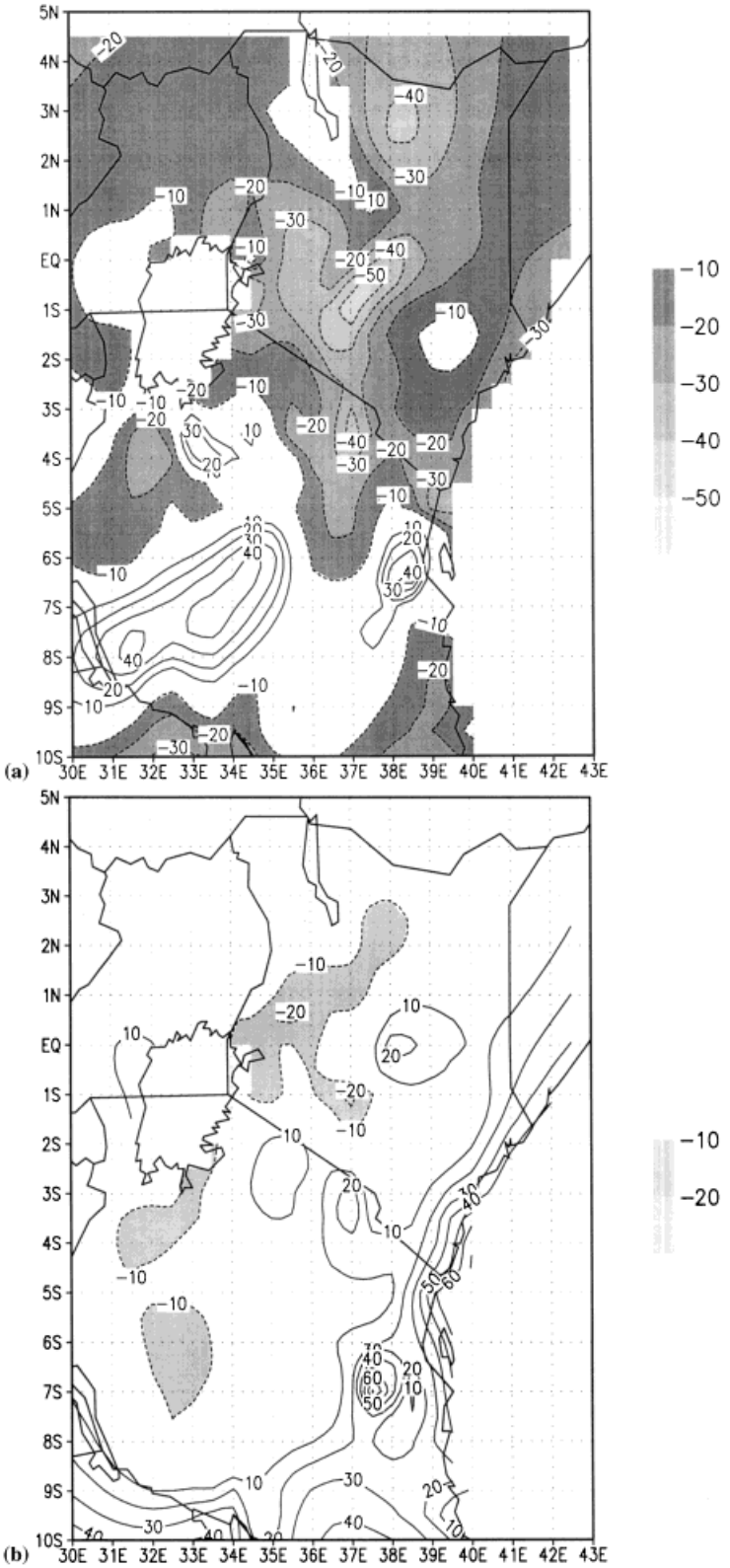

Figure 5. The spatial patterns of the rotated EOF modes for the March–May seasonal rainfall anomalies: (a) first EOF mode and (b) second EOF mode (loading × 100). Values less than − 10 are shaded

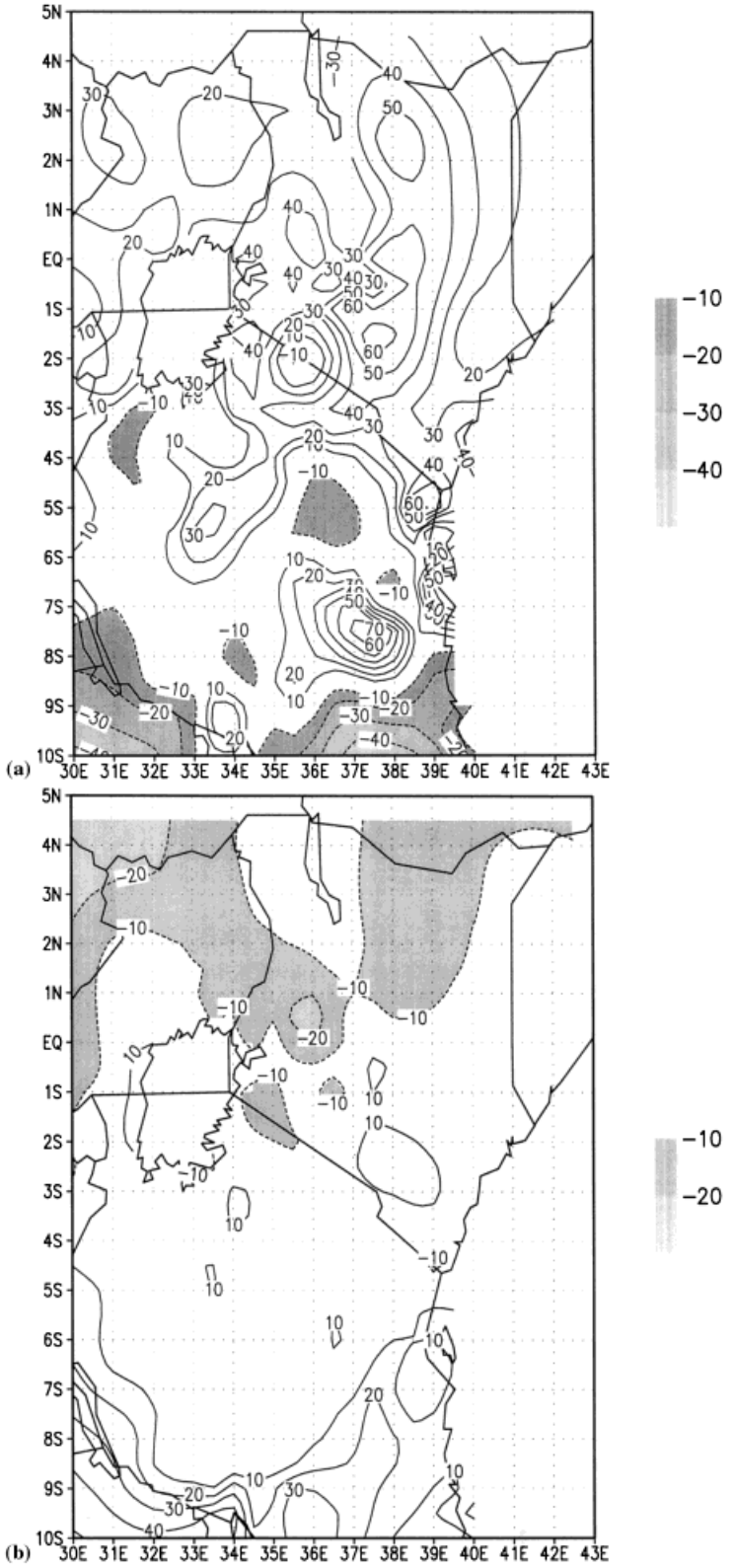

Figure 6. Same as in Figure 5, but for October–December rainfall season

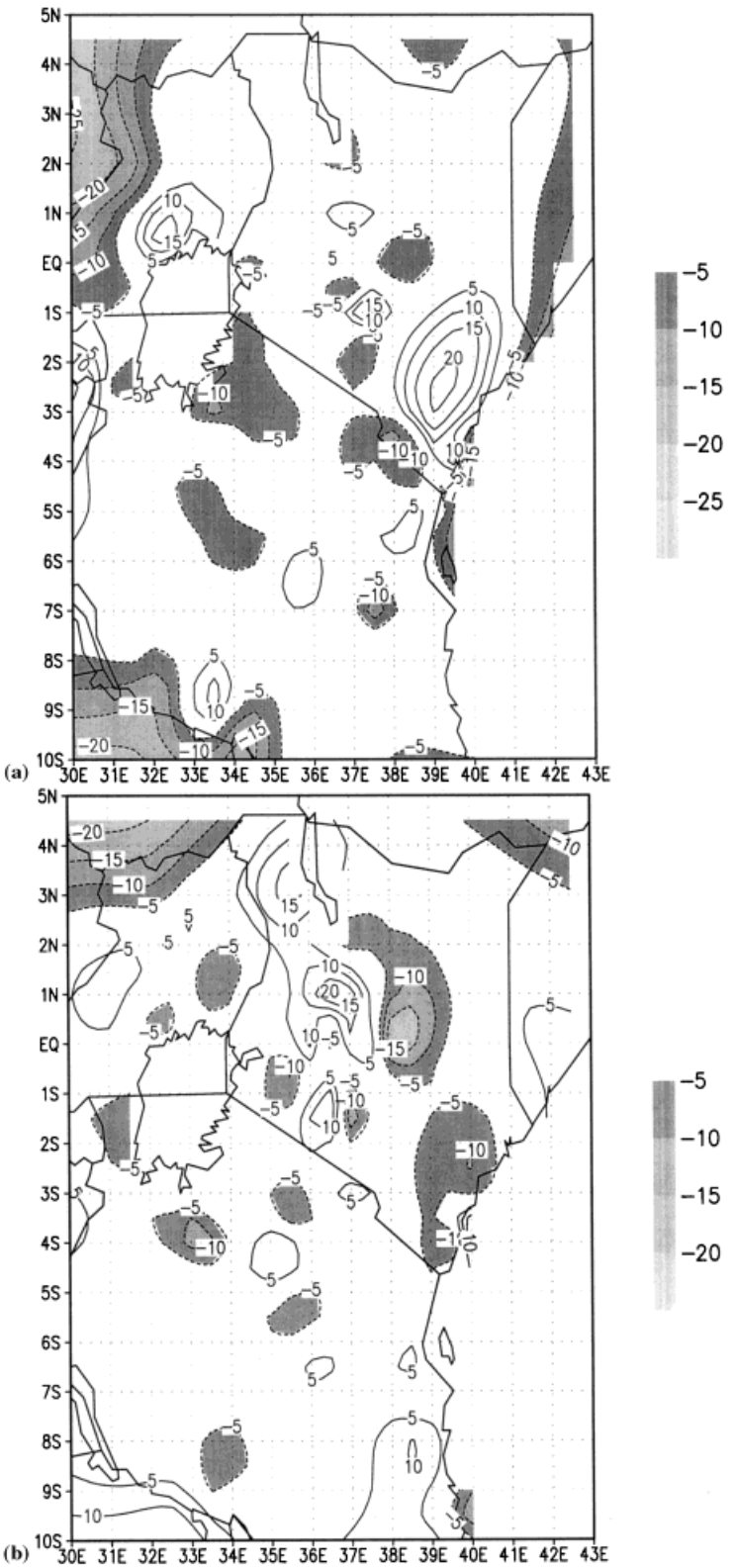

Figure 7. The contour patterns of the rotated eigenvectors for annual rainfall anomalies: (a) first EOF mode and (b) second EOF mode (loading $\times 100$). Values less than -5 are shaded

During the OND rainfall season, the second rainfall EOF mode displays a north/south dipole pattern. This pattern shows that whenever negative rainfall anomalies occur over the southern parts of East Africa, positive rainfall anomalies are experienced over the northern parts the region and vice versa. This configuration may be linked to an ENSO/rainfall dipole pattern (Semazzi and Indeje, 1999) which is highly significant during the OND rainfall season.

The spatial patterns of the first rotated EOF mode for annual rainfall (Figure 7(a)) indicate some concentration of high positive scores over the coastal hinterland of Kenya. The second mode (Figure 7(b)), shows a shift in the high positive scores from the coastal region to the central areas of Kenya. These patterns indicate some likelihood of homogeneous rainfall regions over the coastal areas of East Africa and central Kenya. The principle component score time series provide insight concerning the strength of the EOF patterns over time. Strong amplitudes greater than one standard deviation are observed mainly in the first mode during OND and MAM rainfall seasons (Figures not shown). An extreme score of greater than five standard deviations was observed during the OND season of 1961. This rainfall anomaly event, as indicated by earlier researchers, was associated with the anomalous flow patterns emanating from an unusually warm pool of air over the Indian Ocean (Anyamba, 1984; Reverdin *et al.*, 1986). High positive scores in the first EOF mode were also observed during the years 1963, 1967, 1972, 1977, 1978, 1982 and 1989 during the OND rainfall season. Similarly, during the MAM season, the years 1963, 1967, 1968, 1970, 1977, 1978, 1981, 1985, 1986, 1988 and 1990 displayed low negative scores of less than minus one of the standard deviation, while the years 1961, 1965, 1969, 1971–1973, 1976, 1983–1984 and 1986 displayed high positive scores.

In this study we use annual rainfall anomalies obtained from the mean monthly anomalies in the cluster analysis. Thus, we eliminate the seasonal dependence of the obtained homogeneous rainfall regions over East Africa. It should be noted that Lake Victoria, and southern and western Tanzania, would have more complex spatial rainfall modes during the main rainfall season of March–May (see Figure 5(a)) due to the influence of the complex regional physical features. A further objective was to compare evolutions of ENSO in space and time over homogeneous rainfall regions over East Africa. Hence, the clustered rainfall regions were retained throughout the remaining analyses to enable equal weights to be given to areal rainfall over the different sub-regions of East Africa. The derived EOF rainfall patterns from the annual rainfall anomaly fields (Figure 7) do not give a complete picture of the homogeneous rainfall stations in the region. After correlating the principal components time series and station rainfall time series, eight homogeneous regions were delineated over East Africa: (I) coastal areas of Kenya and Tanzania; (II) eastern highlands of Kenya and Tanzania; (III) central Rift Valley of Kenya; (IV) western highlands of Kenya, northwestern Kenya and northeastern Uganda; (V) central and southern Tanzania; (VI) Lake Victoria region; (VII) central and western Uganda; and (VIII) west of Lake Victoria (Figure 1(b)). The resulting map shows the grouping of stations according to the importance of each eigenvector. The importance of each eigenvector is confined to one specific area of the East African region. In general, the eight regional groupings are similar to the ones constructed by Ogallo (1989). Farmer (1988) found that rainfall over the coastal areas of Kenya (Region I) were highly correlated and could be averaged to form a single rainfall index. Davies *et al.* (1985) analysed rainfall over central Kenya (Region III) and found it to be homogeneous, having a rainfall peak during August when, apart from parts of Uganda, most other parts of East Africa are dry. Eight rainfall time series were constructed corresponding to the sub-regions to be used in the analysis of ENSO/rainfall modulation.

3.3. Composite rainfall map patterns for the ENSO (0) and post-ENSO (+1) onset years

Based on the 30-year ENSO and post-ENSO (+1) rainfall composites, years with normalized rainfall departures greater than +0.2 of the standard deviation were classified as wet rainfall composites, and years with rainfall anomalies less than −0.2 of the standard deviations as dry rainfall composites. The significance of each of these composites was determined by using a variant of the standard *t*-test, which takes into consideration samples with equal variances (Wagner and da Silva, 1994). During the period 1961–1990, there were nine warm El Niño (0) episodes, seven post-ENSO (+1) years and 15 normal

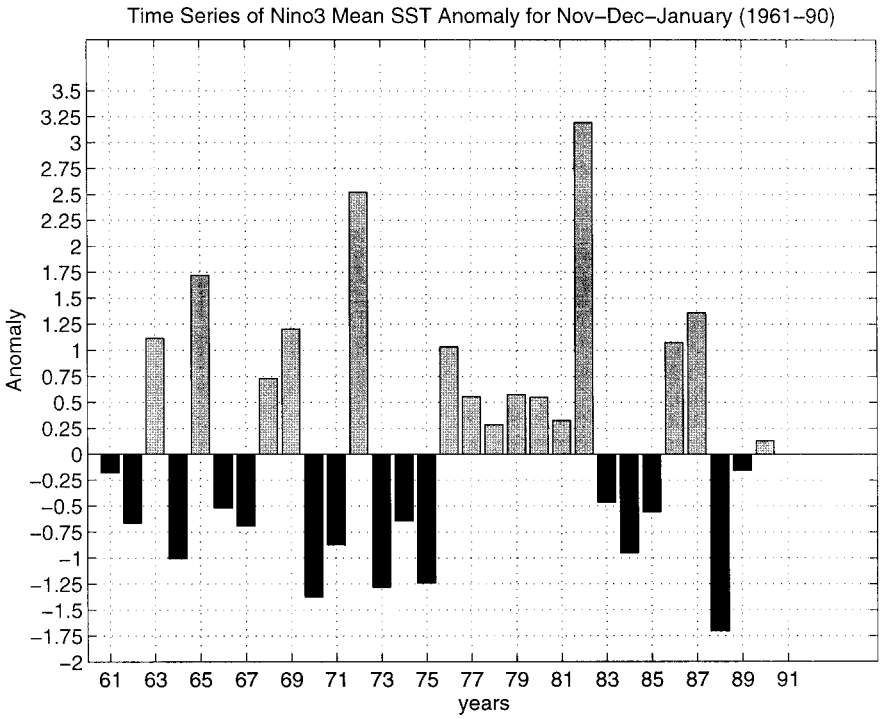

Figure 8. The years with the sea-surface anomaly greater than $+0.75$ are classified warm ENSO and less than -0.75 classified cold ENSO. The years with sea-surface temperature anomalies within this range are classified as normal years (source: Phillips *et al.*, 1998)

years as shown in Figure 8 which are similar to those classified by Trenberth (1997), Phillips *et al.* (1998) and Phillips and McIntyre (1999).

In order to have better understanding of the seasonal mean patterns and the intra-seasonal variability in the rainfall composites, both the mean seasonal and monthly anomaly stratification patterns were analysed. The seasonal rainfall composite map patterns for ENSO onset years (Figure 9), show above normal rainfall conditions over the coastal areas of Kenya and Tanzania (Region I) during MAM. Significantly below normal rainfall is observed over the northern areas of Kenya and Uganda during both the boreal winter and summer seasons. Most parts of East Africa receive normal to above normal rainfall during the 'short rains' season of October–December of the ENSO onset years (Figure 9(d)).

The monthly rainfall map index for the ENSO onset years (Figure 10) for March shows dry conditions experienced in much of the northern parts of East Africa and the lake basin and a few areas over central and southern Tanzania, with the coastal region experiencing relatively wet conditions. During the month of April, dry conditions persist over the central Rift Valley of Kenya and northern Tanzania and significantly high rainfall is observed over the lake basin, central and western Uganda and the East African coast (Figure 10(b)). The results show an east/west dipole pattern in rainfall during the ENSO onset years. A similar pattern was shown by Ogallo (1988) using RPCA on seasonal rainfall patterns over East Africa. During the month of May, wetter than normal rainfall conditions persist over coastal regions, central Uganda and northern Tanzania while dryer than normal conditions are observed over the lake basin, the western highlands of Kenya and southern Tanzania (Figure 10(c)). Wetter than normal conditions are experienced over most of East Africa during the month of June of the ENSO onset years. To summarise, during the ENSO onset years, wetter than normal conditions are to be expected over the coastal areas (Region I) and central Tanzania (Region V) during the 'long rains' season of March–May and, dryer than normal conditions over central Kenya (Region III) and the northern parts of Uganda during the JJAS season. The results further show a tendency for the late onset of the March–May

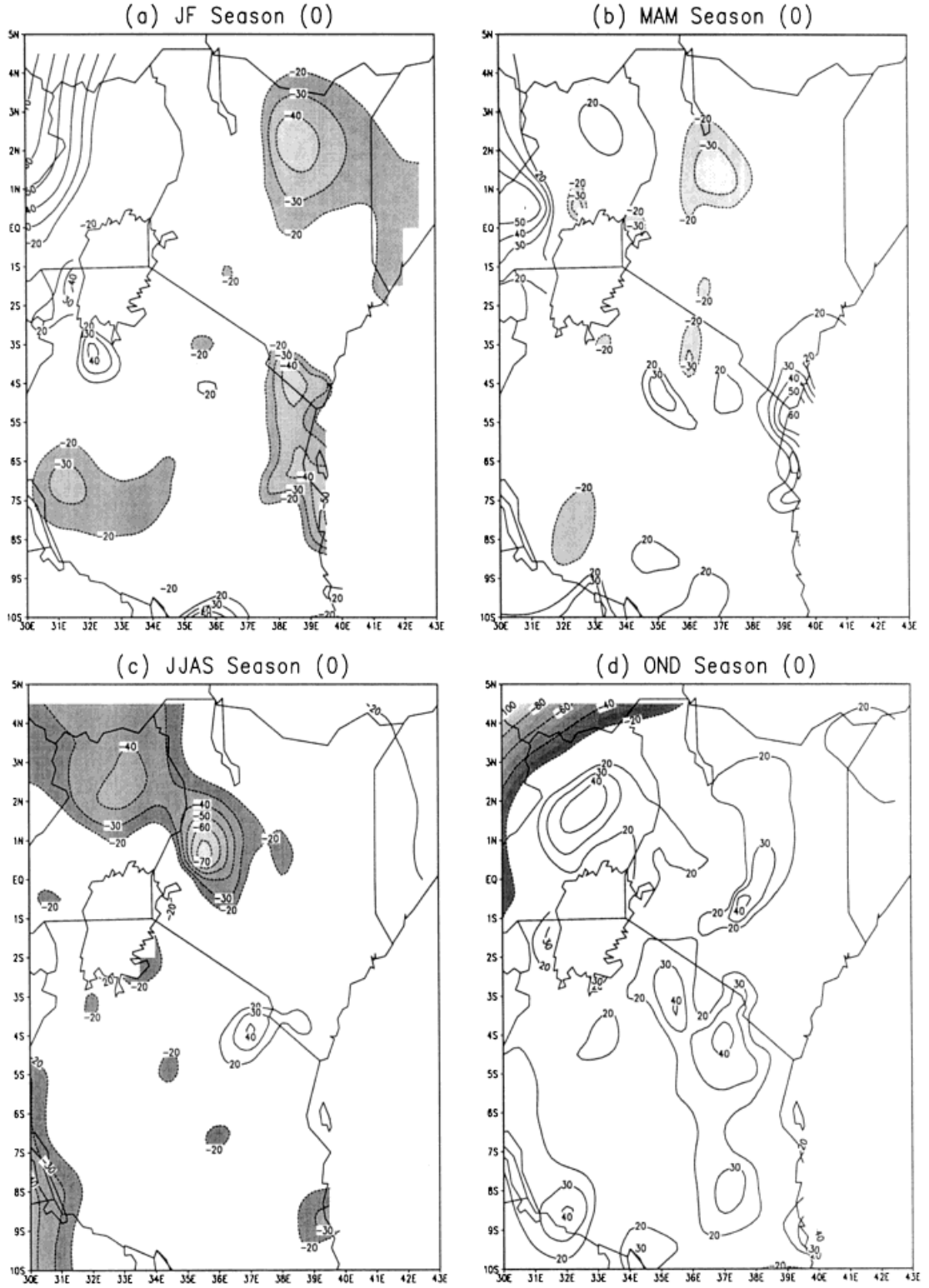

Figure 9. The composite map patterns for seasonal rainfall during the El Niño onset years (loading $\times 100$). The anomalies (20% of the long-term standard deviation are significant at the 5% level. Negative significant anomalies are shaded

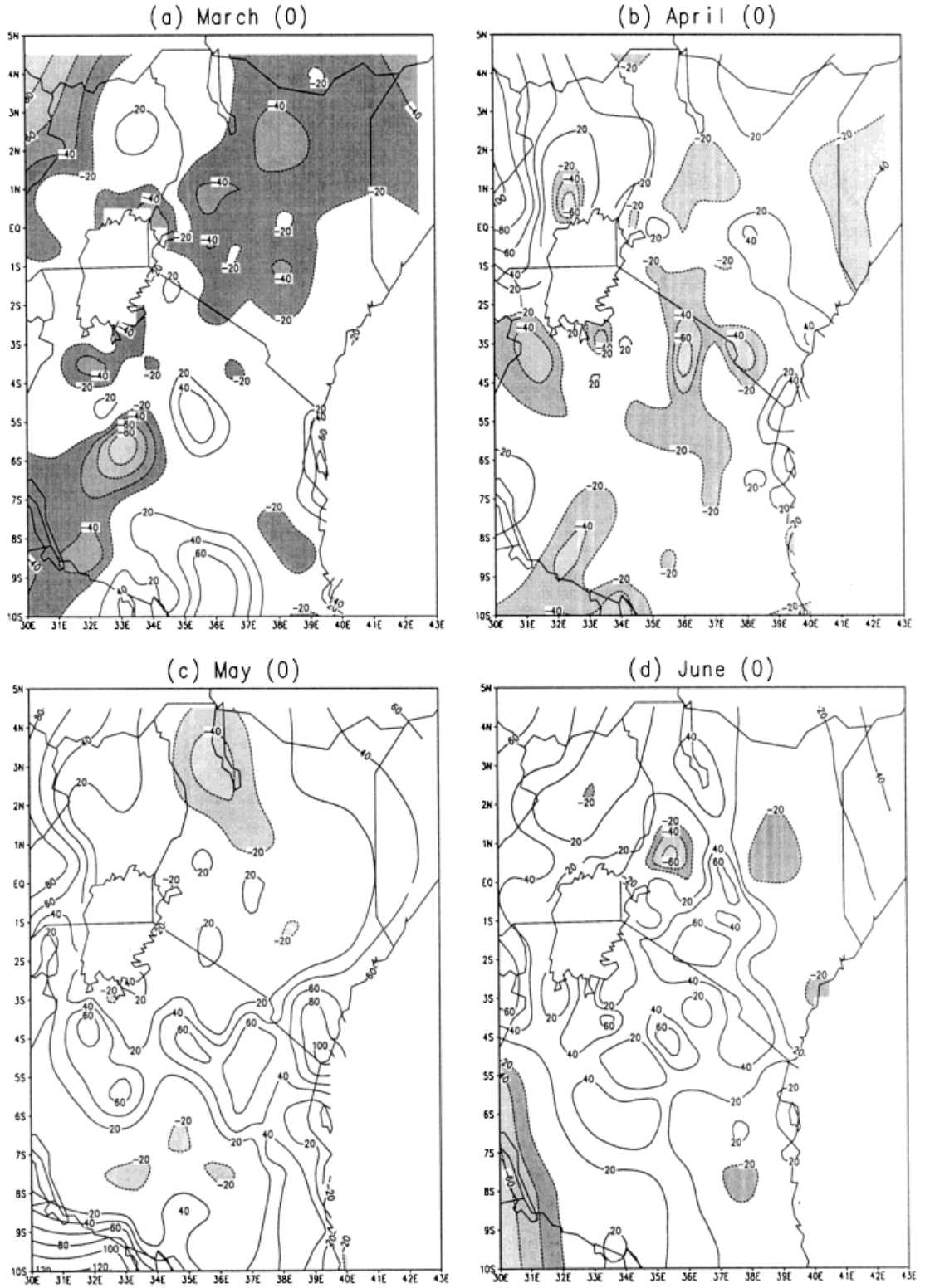

Figure 10. The composite map patterns for monthly rainfall during the El Niño onset years (loading × 100). The anomalies (20% of the long-term standard deviation are significant at the 5% level. Negative significant anomalies are shaded

seasonal rainfall followed by an early cessation over most parts of the northern sector of East Africa during the El Niño onset years.

During the boreal summer period, maximum rainfall is expected over the central Rift Valley of Kenya (Region III) and western highlands of Kenya, northwestern Kenya and northeastern Uganda (Ogallo, 1983; Davies *et al.*, 1985). The rainfall/ENSO composite analysis for seasonal rainfall (Figure 9(c)) is consistent with previous analyses and shows significantly dry conditions over the central Rift Valley, the Lake Victoria basin, northeast Uganda and the western highlands of Kenya during the JJAS rainfall season. Near normal rainfall conditions are observed over most other areas of East Africa. Suppression of the seasonal rainfall peak during the June–September rainfall season may have severe impacts on the soil moisture and agricultural production over the central Rift Valley of Kenya where wheat and barley are widely grown by large-scale farmers. The July–September rainfall peak is as important to the farming community as the 'long rains' of March–May and the 'short rains' of October–December (Davies *et al.*, 1985). The monthly ENSO/rainfall composite for this season (Figures not shown) shows persistent dry conditions over these regions during the entire June–September rainfall season.

The ENSO/rainfall index for the months of September–December of the ENSO onset years are shown in Figure 11. The Figure shows continuing dry conditions over the western highlands of Kenya and northeastern Uganda, the central Rift Valley of Kenya, parts of the Lake Victoria basin and parts of central Tanzania during September. Wetter than normal rainfall conditions are experienced over northeastern Kenya and parts of northern Tanzania during this month. During October, most regions of East Africa receive normal to above normal rainfall conditions with high rainfall observed over central Tanzania. During November and December, wetter than normal rainfall conditions are experienced over the eastern highlands, central Uganda, the lake basin and the coastal regions (Figure 11(c and d)). Dryer than normal conditions are experienced over the southern parts of Tanzania and some parts of the East African coast during this period. There is a sudden reduction of rainfall over the coastal areas during December (Figure 11(d)), but wetter than normal conditions are still experienced over most parts of East Africa. The sudden cessation of rainfall and switch from wet (November) to dry conditions in December over the coastal area can have devastating impacts on the soil moisture and hence on agricultural production in these areas. Farmer (1988) noted the importance of the 'short rains' of October–December in maintaining fruit and vegetables over the coastal areas of Kenya. These results suggest that most areas of East Africa are prone to relatively wet rainfall conditions during the October–December of the ENSO onset years.

The seasonal rainfall composite maps for the post-ENSO (+ 1) years (Figure 12) indicate wet rainfall conditions over most parts of East Africa during the JF rainfall season. The relatively wet conditions during the 'short rains' of OND tend to extend to the following year and are mainly responsible for the wet conditions observed during this season. Dry conditions are observed over southern Tanzania during the MAM season (Figure 12(b)). The monthly ENSO/rainfall composite map patterns for the post-ENSO (+ 1) years (Figure 13) show dry conditions in March over the western highlands of Kenya and southern parts of the coastal region and wetter than normal conditions over central Tanzania, the eastern highlands of Kenya, the lake basin and northwestern Uganda. During April, wetter than normal rainfall conditions are observed over the Lake Victoria basin and some parts of northern Tanzania, and significantly dry conditions over central and southern Tanzania and southern parts of the East African coast. Most areas of East Africa receive significantly below normal rainfall conditions during May in the post-ENSO (+ 1) years (Figure 13(c)) except for a few areas over the western highlands of Kenya, central Rift Valley of Kenya and central Tanzania which receive near normal rainfall conditions. Near normal rainfall conditions are received in most parts of East Africa during the month of June of the post-ENSO (+ 1) years.

During the northern hemisphere summer season, wetter than normal rainfall conditions are experienced over the western highlands and central Rift Valley of Kenya, and northeastern Uganda (Figure 12(c)) as opposed to the extremely dry conditions observed during the ENSO onset years. These results suggest the existence of a negative correlation between the June–September rainfall over these regions with ENSO. Dry conditions are experienced over the Kenyan coast and parts of northern Tanzania during this season.

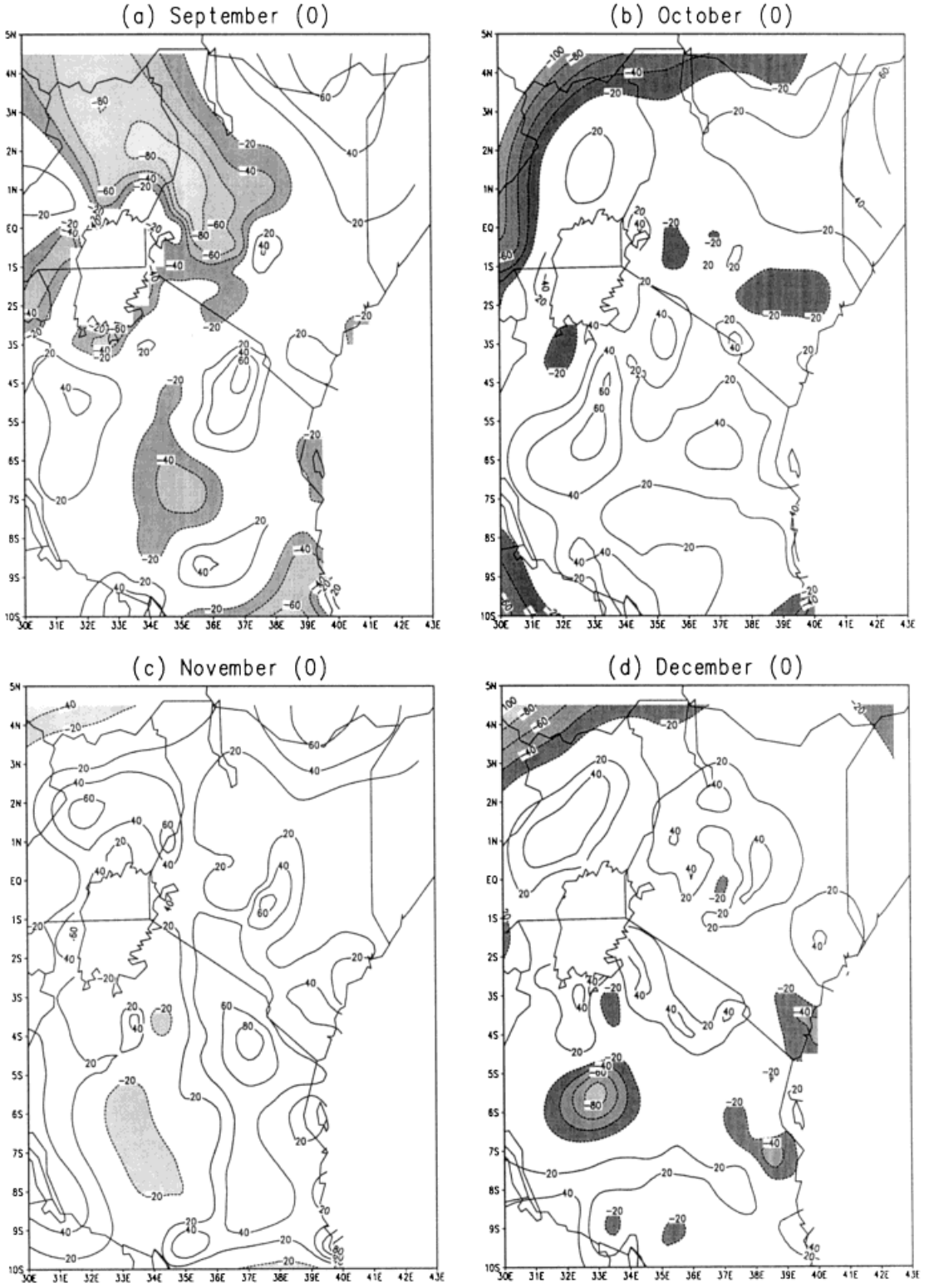

Figure 11. Same as in Figure 10, but for different months

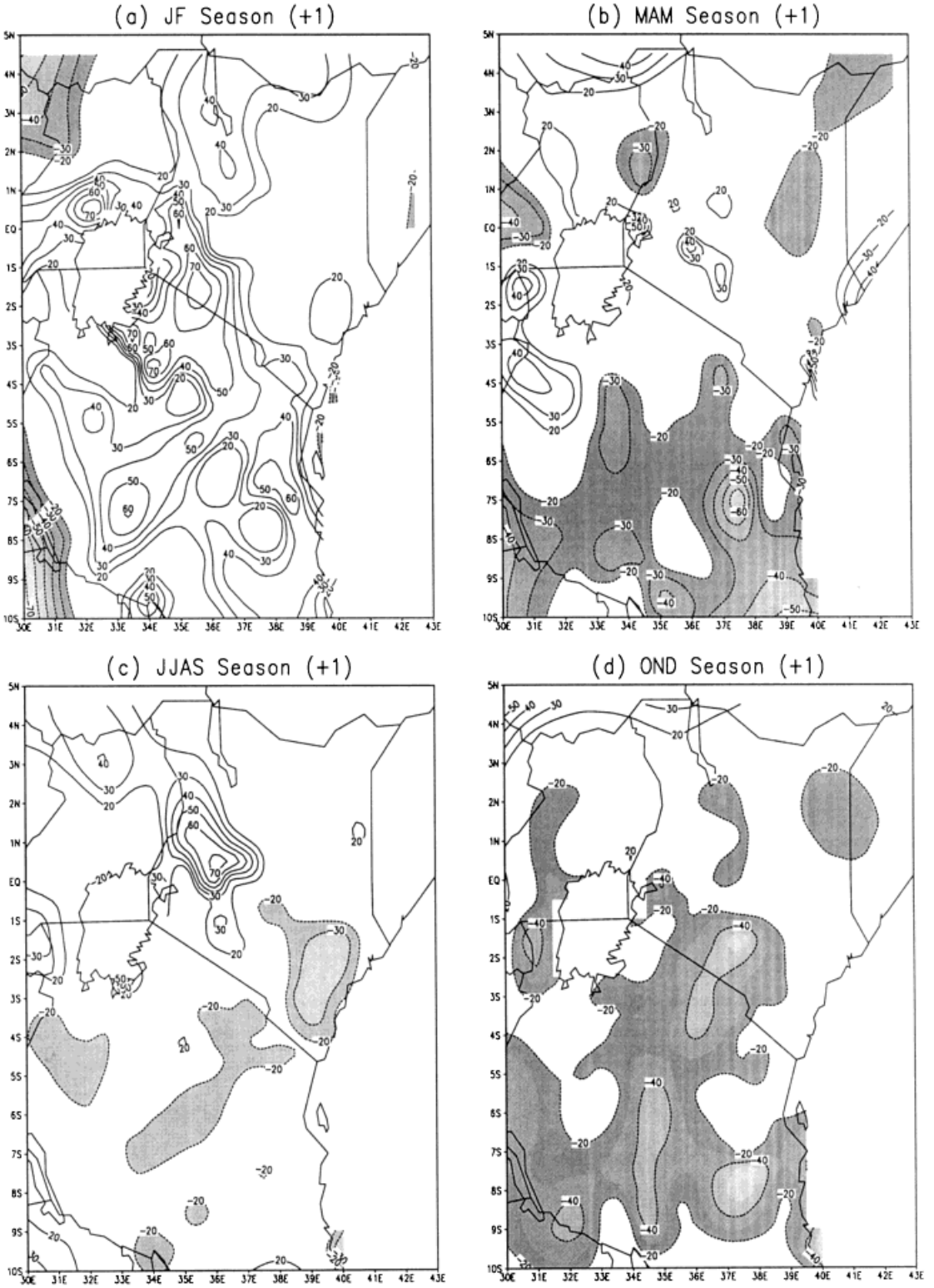

Figure 12. Same as in Figure 9, but for post-ENSO (+ 1) years

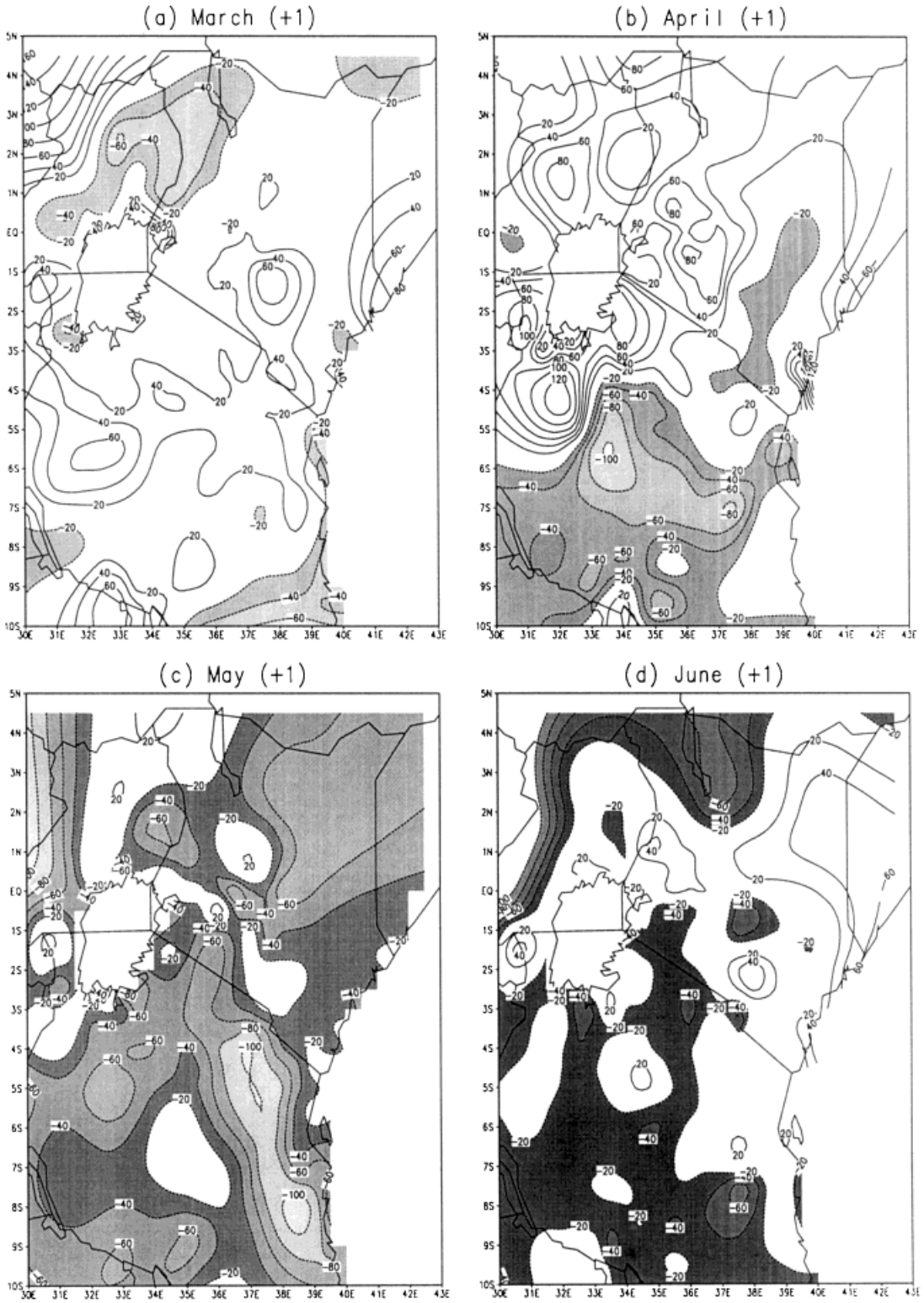

Figure 13. The composite map patterns for monthly rainfall during the post-ENSO (+ 1) years (loading × 100). The anomalies (20% of the long-term standard deviation are significant at the 5% level. Negative significant anomalies are shaded

Since rainfall in this season is crucial for the farming community in the central Rift Valley, and western highlands of Kenya, the lake basin and central Uganda, advanced knowledge of the expected timing and performance of the rainfall season could be very important for agricultural and other socio-economic planning in the region.

The East African region experiences the second passage of the ITCZ as it progresses from north to south during the October–December period. Over most parts of East Africa, this rainfall season is important to the farming community for maintaining cash crops such as tea, coffee and corn. This rainfall season is also important in maintaining the growth of Savannah grasslands and shrubs over parts of the eastern highlands of Kenya and northern Tanzania where wildlife animals in National Parks are a tourist attraction. The results obtained from the post-ENSO ($+1$)/rainfall composite maps for this season (Figure 12(d)) shows significantly dry conditions over the eastern highlands of Kenya, the Lake Victoria basin, western Uganda and central Tanzania. The rainfall deficit creates unfavorable conditions for grazing and for crop growth and development. Advanced knowledge of the timing and the expected performance of this rainfall season could be of much benefit to the farming community for planning the schedule of planting and crop rotation. The monthly rainfall composite map patterns (Figure 14) show persistent dryer than normal rainfall conditions over East Africa during October to December, but there is significantly high rainfall over the central Rift Valley of Kenya, the western highlands of Kenya and northeastern Uganda, and the Lake Victoria basin during September (Figure 14(a)). Areas over the eastern highlands of Kenya and the coastal areas of East Africa recover from the dry conditions in the early part of the season during the wetter month of December (Figure 14(d)).

The earlier work by Ropelewski and Halpert (1987) showed a dipole ENSO/rainfall pattern over eastern and southern Africa. Wetter than normal conditions were indicated over eastern Africa and drier conditions over southern Africa during ENSO years. Whilst Nicholson (1996) indicated that there is a tendency for rainfall to be above average for most parts of East Africa during ENSO years and for drought to occur during the following year. One of the major results of the detailed inspection of the rainfall anomaly patterns described here is to reveal a more complicated distribution of rainfall anomalies over eastern Africa than the simple dipole cited earlier. Our results elaborate in detail the earlier ENSO/rainfall work done over the region and are important for the long-range seasonal rainfall monitoring and guidance in the East African region based on prior information of the expected ENSO events. Once the onset of an El Niño event is ascertained either by empirical or numerical prediction techniques, then it will be possible to use the results obtained from our ENSO/rainfall composite maps to monitor and provide guidance on the likely evolution of the rainfall anomaly patterns over different regions of East Africa.

3.4. Observed shifts in the seasonal rainfall cycle induced by ENSO

The seasonal rainfall cycle for each of the eight regions of East Africa was analysed for mean climatology, ENSO onset and post-ENSO ($+1$) years to detect shifts in the rainfall seasons between the three groupings and to speculate on possible socio-economic impacts. It should be noted that besides the modulation of rainfall due to ENSO, which accounts for about 50% of the East African seasonal rainfall variance (Ogallo, 1988), there are other important factors which influence East African rainfall variability. These include the Quasi-Biennial Oscillation (Ogallo *et al.*, 1994) and the 30–60 day Julian–Madden tropical wave (Anyamba, 1990). Nicholson (1996) has noted that East African rainfall is clearly linked to large-scale features of general circulation including sea-surface temperatures. Camberlin (1995) and Mutai *et al.* (1998) have shown significant relationships between rainfall over East Africa and the atmospheric flow patterns over the region. In this study we are confining our analysis to the association of ENSO with the East African regional rainfall.

The mean seasonal pattern for the East African coastal areas (Region I) shows the expected bimodal rainfall distribution with the rainfall peaks observed in April–May and November (Figure 15(a)). An early onset of rainfall is shown during ENSO. The rainfall in April–May is greater than in normal years. During the post-ENSO ($+1$) years there is a timely onset of the March–May rainfall season followed by

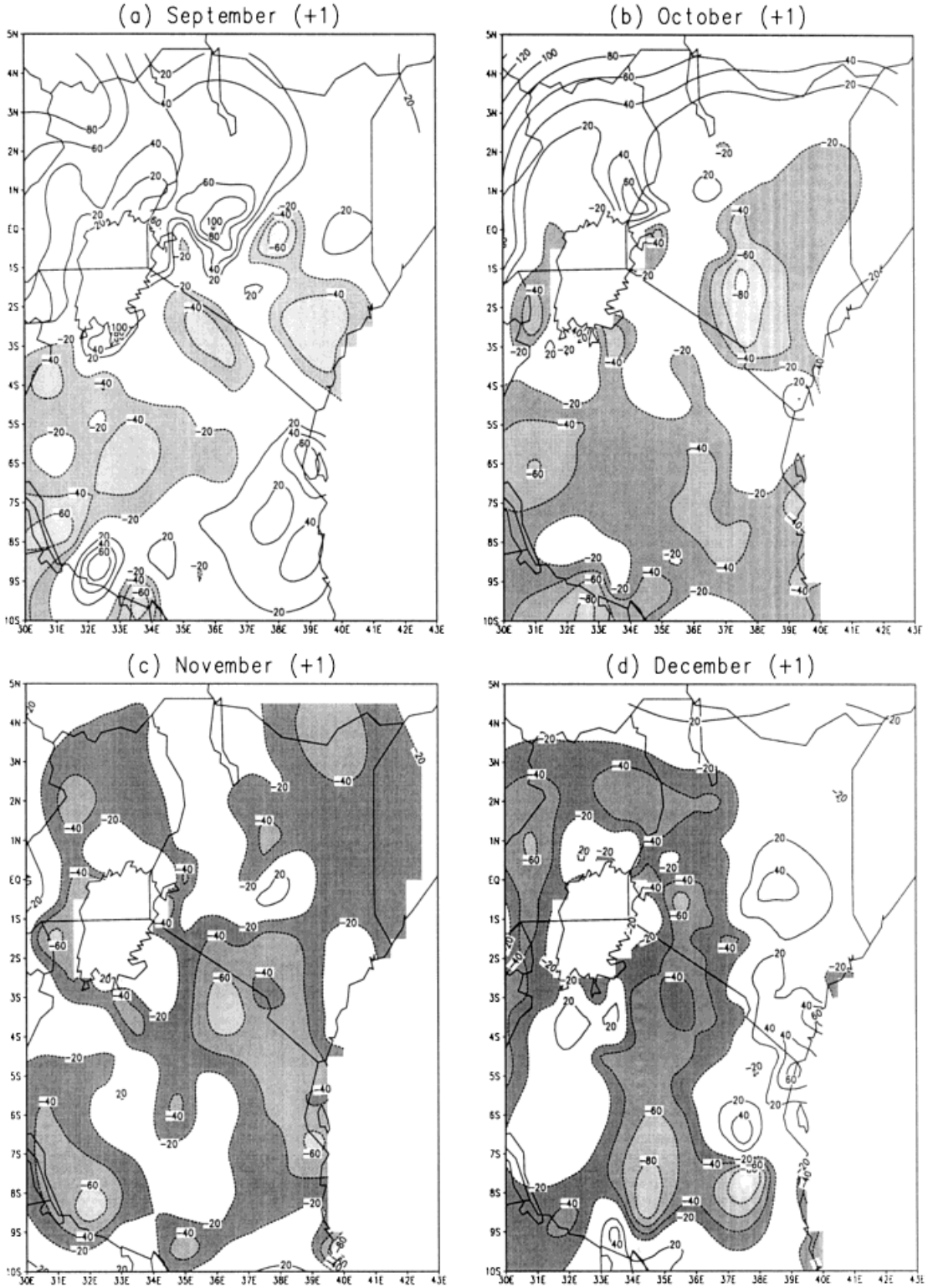

Figure 14. Same as in Figure 13, but for different months

an early cessation. During the short rains of October to December in ENSO onset years, there is significantly high rainfall with a peak in November well above the climatological mean. In post-ENSO (+ 1) years, there is relatively poor performance of short-season rains and a shift in the rainfall maxima to December instead of November as is usually expected. Early knowledge of seasonal performance and any expected shift in the seasonal rainfall over these regions would be important for agricultural planning of fruit and vegetables. Prolongation of both long and short rains during ENSO onset years can be relatively important in maintaining soil moisture and therefore the performance of crops. On the other hand, early cessation of the long rains during post-ENSO (+ 1) years and a shift in the rainfall maxima from November to December would affect the different growing stages of crops and affect yield. Farmers might benefit from late planting under such conditions, although other factors would have to be taken into account.

In Region II, covering most parts of the highlands east of Rift Valley, normal performance of the long rains is indicated during the ENSO onset years. During the post-ENSO (+ 1) years, there is an early onset of the long rains, which become more intense surpassing the long-term mean (Figure 15(b)). There is normal timing in the short rains during both the ENSO onset and the post-ENSO (+ 1) years. However, there are noticeable differences in rainfall performance, with wet conditions occurring during ENSO onset years and relatively dry conditions during post-ENSO (+ 1) years. Crops planted which are dependent on the March–May rainfall season are expected to perform normally during both the ENSO onset and

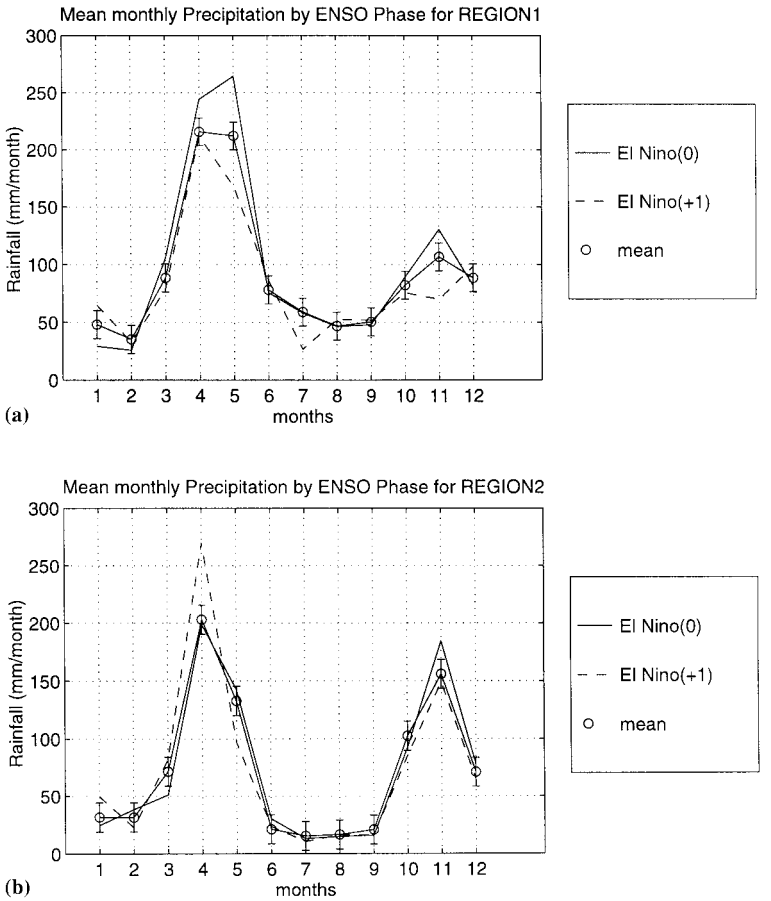

Figure 15. The mean monthly precipitation by ENSO phase for the eight homogeneous rainfall regions over East Africa. The error-bar on the mean climatological annual rainfall cycle represents ± 20% of the climatological monthly mean. Values outside ± 20% of the long-term mean are significant at the 5% level

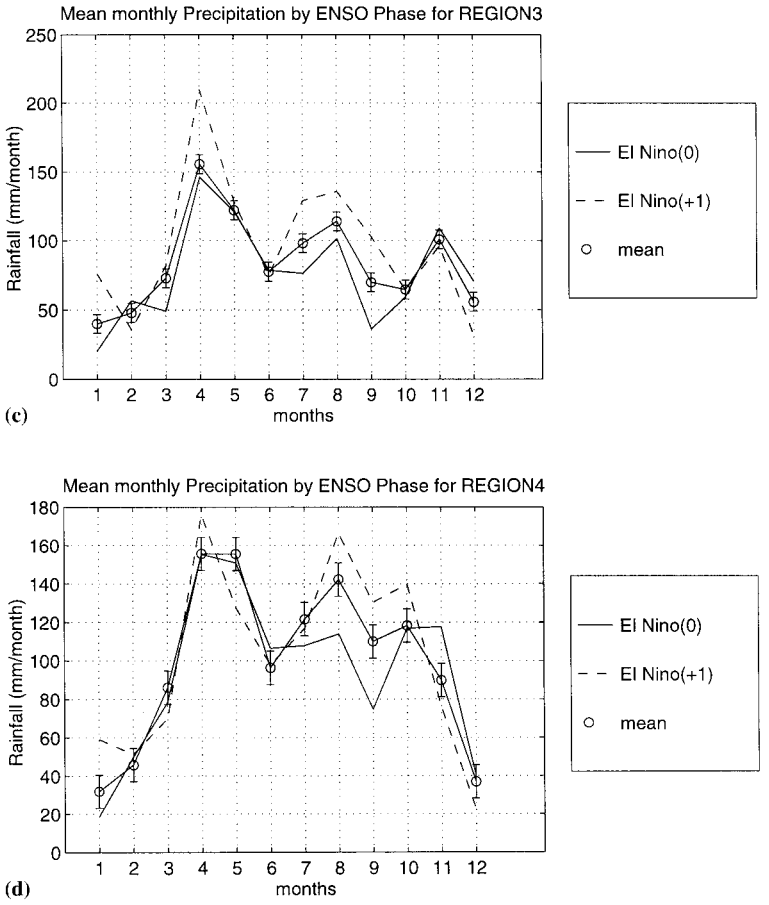

Figure 15 (*Continued*)

post-ENSO (+ 1) years, but to experience later moisture stress during the post-ENSO (+ 1) years followed possibly by poor harvests.

The effect of an ENSO episode on the seasonal rainfall cycle over the central Rift Valley of Kenya (Region III) is shown in Figure 15(c). The Figure shows that during ENSO onset years, there is a late onset of the long rains followed by an early cessation. During the post-ENSO (+ 1) years, there is an early onset of long rains and rainfall peak reached normally in April. However, significantly wet conditions, well above the long-term mean, are experienced during this season. During ENSO years, the expected rainfall peak in August is significantly diminished. Such suppression of mid-year rains could have a severe impact on agricultural production in a region where both large-scale and subsistence farmers grow wheat and maize and depend on this rainfall season. During the post-ENSO (+ 1) years, there is a normal onset of July–September rainfall with very wet conditions that persist and link-up with the short rains season of October–December. There is a late onset but late cessation of the October–December rains during the ENSO onset years. During post-ENSO (+ 1) years a normal onset is followed by an early withdrawal.

The impacts of ENSO on rainfall over the western highlands of Kenya, northwestern Kenya and northeastern Uganda (Region IV) is shown in Figure 15(d). It can be seen that during ENSO years there is a late onset and a poor seasonal rainfall performance of the March–May rains. During post-ENSO (+ 1) years, the indicated early onset of rainfall attains a normal maxima in April as expected but is significantly higher than the long-term mean. Advance guidance regarding the expected shift in the rainfall season due to ENSO will be crucial for socio-economic planning in this region which depends on the long

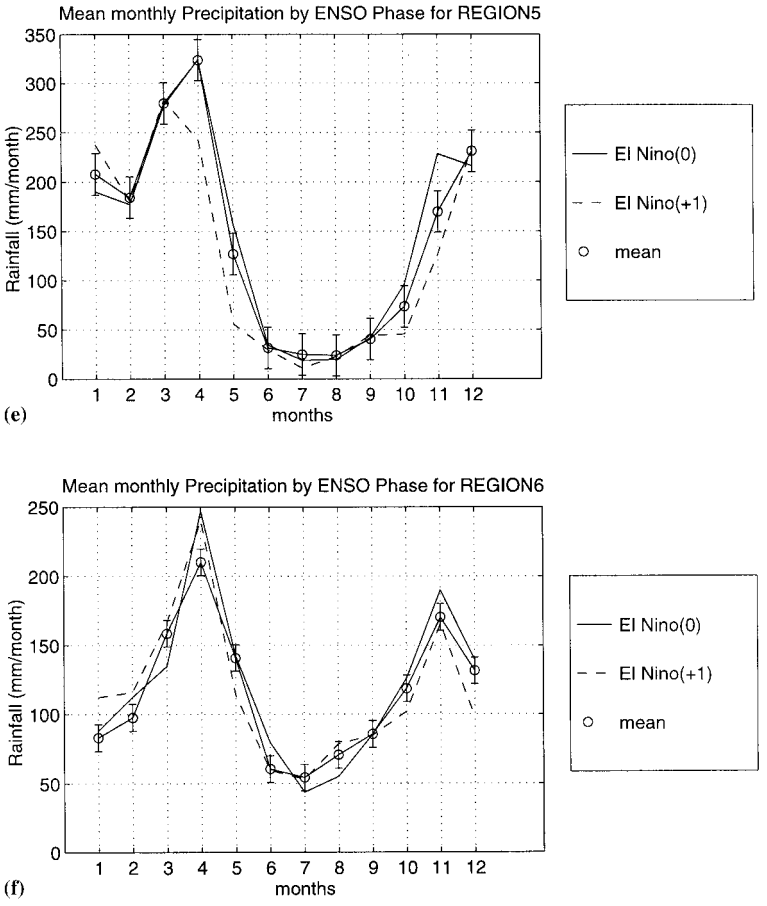

Figure 15 (*Continued*)

rains for agricultural production of maize by both large-scale and subsistence farmers. Based on climatological information alone, if the farmers were advised to delay planting by a month or so, it could be beneficial to the final yield. During ENSO onset years, the short rains tend to perform normally with better than average rainfall in November. In post-ENSO (+ 1) years, relatively high rainfall is experienced during July–October with poor rainfall performance during the short rains of November–December. Since evaporation rates are high during July–September, the poor performance of the late short rains may result in failure to sustain soil moisture. Beans and potatoes planted during this period are likely to produce poor yields.

The mean monthly precipitation by ENSO phase for central and southern Tanzania (Region V) is shown in Figure 15(e). Apart from rainfall suppression during post-ENSO (+ 1) years and significantly high rainfall anomalies during the ENSO onset years during the main rainfall season of October–May, there is no significant shift in the pattern of seasonal rainfall. The socio-economic implications of ENSO in this region may be felt due to the persistence of dryer than normal conditions during post-ENSO (+ 1) years. Crops grown during the normal growing season will experience significant moisture stress with less rainfall for normal agricultural production. It would be advantageous for farmers to plant alternative crops, which require little rainfall and soil moisture to mature.

Figure 15(f) shows the mean monthly precipitation by ENSO phase for the Lake Victoria basin (Region VI). The Figure shows that during ENSO onset years, there is a late onset of the long rains of March–May. An early onset followed by significantly high rainfall during April but an early withdrawal of the seasonal rainfall during post-ENSO (+ 1) years is indicated. Late planting would be recommended

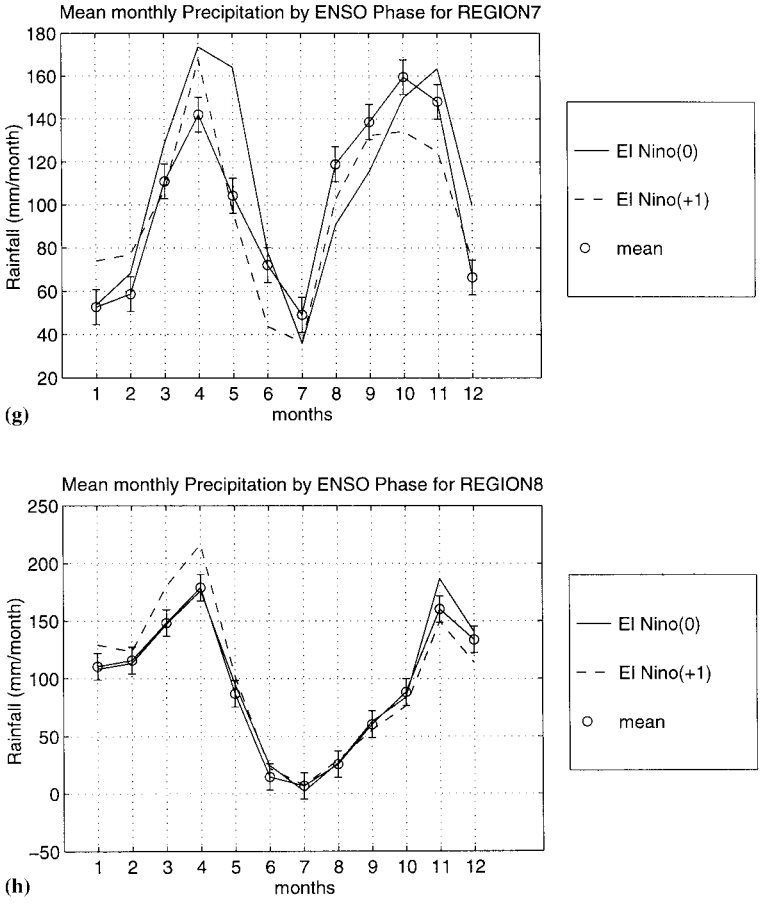

Figure 15 (*Continued*)

for the ENSO onset years to coincide with the late onset of the seasonal rainfall. The Figure also shows that during ENSO onset years, the normal increase of rainfall in August in this region is suppressed. Any crop, which depends on this seasonal rainfall to mature, is likely to do poorly during ENSO years. The high rainfall experienced during December of the ENSO onset years may not be sufficient to replenish and sustain the soil moisture and the crops usually grown in this region since the preceding season is dry. Alternative crops requiring less soil moisture and rainfall to mature may be a suitable alternative for this region during ENSO episodes.

The mean monthly precipitation by ENSO phase for central and western Uganda (Region VII) is shown in Figure 15(g). The Figure shows a near normal onset of the March–May seasonal rainfall during ENSO years, followed by a late withdrawal and a significantly high seasonal rainfall giving normal to above normal rainfall conditions. On the other hand, there is a normal onset of long rains during the post-ENSO (+ 1) years, but with a peak in April followed by an early withdrawal in May indicating a shortened rainfall season. This can have severe impacts on regional soil moisture. The results show further that during the short rains there is an earlier onset during the post-ENSO (+ 1) years than during the ENSO onset years. During the ENSO onset years, above normal conditions are observed in a late November peak, followed by a normal rainfall withdrawal. During the post-ENSO (+ 1) years, the early onset is followed by an early below normal maximum in September–October as opposed to October–November, followed by early withdrawal. This drastic shift and reduction in the short rains during post-ENSO (+ 1) years can have severe impacts on agriculture. The rainfall comes before the farmers have prepared for the next planting. On the other hand, if the heavy rainfall is received during harvest

time for the first crop, especially for maize, which is usually harvested at this time of the year, it may impact on yield due to the presence of high air moisture. If farmers are advised of the impending seasonal climate conditions in advance, they have an opportunity for formulating alternative remedies. One alternative would be to plant only once and late into the rainfall season.

Figure 15(h) which shows the effect of ENSO on seasonal rainfall over the area west of Lake Victoria (Region VIII), indicates that, during ENSO onset and post-ENSO (+ 1) years, there is not much shift in the long rains, but high rainfall is observed during post-ENSO (+ 1) years and poor rainfall during the ENSO onset years. During the ENSO years, the October–December seasonal rainfall sets in normally although in post-ENSO (+ 1) years there is an early cessation and a generally poorer rainfall performance. The reliability of this rainfall season should ensure the maintenance of conditions and healthy crop performance. However, early planting during post-ENSO (+ 1) years would appear to be a prudent strategy.

4. CONCLUSIONS AND DISCUSSION

The results obtained in this study show large spatial and temporal variability in seasonal rainfall through the 30-year period (1961–1990). These results are consistent with earlier studies by Ogallo (1980), Beltrando (1990), Nyenzi (1990) and Nicholson (1996). Results obtained from the EOF analysis of the seasonal rainfall show patterns that resemble the mean climatology, which is primarily dictated by the seasonal migration of the ITCZ as indicated in the first EOF mode (Figures 5(a) and 6(a)). The interactions between the prevailing easterly flow and the meso-scale circulations that play a major role in the diurnal and intra-seasonal rainfall variability in the region were clearly discernible in the second dominant EOF rainfall mode (Figures 5(b) and 6(b)). There was an indication of contributions, which may be associated with rainfall generating systems such as easterly waves, and a 30–60-wave oscillation, in the third EOF modes. The principal component time series showed years that experienced floods/droughts during the study period, 1961 having the highest amplitude of more than five standard deviations.

Application of rotated EOF and simple correlation analyses yielded eight homogeneous rainfall regions in East Africa. Dyer (1977) used a similar approach for South Africa. Our homogeneous regions compare well with those obtained by earlier researchers (Nicholson *et al.*, 1988; Ogallo, 1989, among others) and are reasonable in spatial distribution. These homogeneous rainfall regions will be useful in the formulation of empirical rainfall forecasting models for the eight regions and in verifications of regional climate model results over the East African region.

The results further confirm the identification of relationships between seasonal rainfall in East Africa and phases of ENSO. The results show, however, that not all areas/seasons of East Africa are wet/dry during the El Niño/post-ENSO (+ 1) years as usually claimed. Relatively wet conditions were observed during the March–May and October–December rainfall seasons of the El Niño years. Similar results were obtained during June–September of the post-ENSO (+ 1) years. Dry conditions dominate in June–September of the El Niño onset years and the two seasons (March–May and October–December) of the post-ENSO (+ 1) years. The results also delineate areas that are prone to excess/deficit rainfall during the El Niño/post-ENSO (+ 1) years. These results agree with the findings of Nicholson (1996) that there is a tendency for rainfall to be above average in most parts of East Africa during ENSO years and for rainfall deficits to occur during the following year, with positive rainfall anomalies occurring during the short rains of the ENSO year. Our findings do not agree with her suggestion of negative anomalies during the long rains of the following year except in southern Tanzania.

Our results have shown that ENSO plays a significant role in determining the monthly and seasonal rainfall patterns in the East African region. In some regions there are shifts in the onset/cessation of rainfall while in others there is a significant reduction in the seasonal rainfall peak during ENSO/post-ENSO (+ 1) years. For instance the June–July to August rainfall season over the central Rift Valley of Kenya (Region III) is significantly diminished during the ENSO onset years. The suppression of this

seasonal rainfall can have severe socio-economic impacts especially on agriculture. The June–September rainfall maintains the different growing stages of crops especially wheat planted by both large-scale farmers and small-scale peasant farmers in the region. Advanced knowledge of the expected seasonal rainfall performance in association with ENSO and other factors, and fast dissemination of the climate information to farmers, could be highly beneficial. These results show in detail the effects of ENSO in shaping the seasonal rainfall patterns over East Africa postulated by earlier researchers (Ropelewski and Halpert, 1987; Ogallo, 1989; Nicholson, 1996, among others). Using a longer rainfall time series having more ENSO/rainfall composites may make the results more robust. Also, a higher frequency temporal analysis based on daily or 5-day rainfall (pentads) would prove useful in identifying the likely onset of seasonal rainfall and the planting dates. This analysis could be performed in any region where rainfall is influenced by different phases of the ENSO cycle. The results obtained from this study have direct applications in operational seasonal rainfall monitoring and prediction for East Africa.

ACKNOWLEDGEMENTS

Part of this work was supported by the International Research Institute (IRI)/NOAA Global Projects. The authors are indebted to Professor Mark Cane for his valuable discussions and the African Centre for Meteorological Applications and Development (ACMAD) for nominating the first author to participate in the International Institute for Climate Predictions pilot project at Lamont Doherty Earth Observatory of Columbia University, New York. The later part of this research was supported by the NSF/Climate Dynamics Program grant # ATM-9424289. The computations were performed on the North Carolina Super Computing Center (NCSC) Cray-YMP and on the FOAM^{V} visualization and parallel computing facility at NCSU, which is supported by IBM. Any opinions, findings and conclusions or recommendations expressed in this material are those of the authors and do not necessarily reflect the views of the IBM Corporation. We extend our gratitude to P. Ambenje of the Drought Monitoring Center (Nairobi) and the Director of the Kenya Meteorological Department for providing the rainfall data. We acknowledge the enlightening discussions with L. Xie, G. Pouliot, L. Sun, Y. Song and X. Bowei and their help during the various stages of this work. We are also grateful to the anonymous reviewer who did an excellent job in improving the text.

REFERENCES

Alusa, A.L. 1976. 'The occurrence and nature of hailstorms in Kericho, Kenya', *Proceedings of the WMO/IMAP 2nd Scientific Conference on Weather Modification*, Boulder, Colorado, 2–6 August, 1976, pp. 249–256.

Anderson, T.W. 1963. 'Asymptotic theory for principal component analysis', *Ann. Math. Stat.*, **34**, 122–148.

Anyamba, E.K. 1984. 'Some aspects of the origin of rainfall deficiency in East Africa', *Proceedings of the WMO Regional Scientific Conference on GATE, WAMEX and Tropical Meteorology*, Dakar, Senegal, pp. 110–112.

Anyamba, E.K. 1990. *A diagnostic study of low frequency oscillations in tropical Out Going Longwave Radiation*, PhD Dissertation, University of Nairobi, Nairobi, Kenya, 190 pp.

Asnani, G.C. and Kinuthia, J.H. 1979. *Diurnal Variation of Precipitation in East Africa*, E. Africa Meteorol. Dept., Memo., 8, 58 pp.

Atwoki, K. 1975. 'A factor analytic approach for the delimitation of the rainfall regions of Uganda', *East African Geogr. Rev.*, **13**, 9–36.

Barring, L. 1988. 'Regionalization of daily rainfall in Kenya by means of common factor analysis', *J. Climatol.*, **8**, 371–389.

Beltrando, G. 1990. 'Space-time variability in April and October–November over East Africa during the period 1932–1983', *J. Climatol.*, **10**, 691–702.

Barnett, T.P. and Davies, R.E. 1975. 'Eigenvector analysis and prediction of sea surface temperature fluctuation in the northern Pacific Ocean', *Proceedings of the WMO/IAMAP Symposium on Long-term Climatic fluctuations*, Norwich, England, pp. 439–450.

Camberlin, P. 1995. 'June–September rainfall in northeastern Africa and atmospheric signals over the tropics: a zonal perspective', *Int. J. Climatol.*, **15**, 773–783.

Cane, M., Zebiak, S.E. and Donald, S.C. 1986. 'Experimental forecasts for El-Niño', *Nature*, **321**, 827–702.

Davies, T.D., Vincent, C.E. and Beresford, A.K.C. 1985. 'July–August Rainfall in west-central Kenya', *J. Climatol.*, **5**, 17–33.

Dyer, T.G.J. 1977. 'The assignment of rainfall stations into homogeneous groups: An application of principal component analysis', *Q. J. R. Meteorol. Soc.*, **101**, 1005–1013.

Dyer, T.G.J. 1981. 'On the interannual variation in rainfall over the sub-continent of Southern Africa', *J. Climatol.*, **2**, 47–64.

Farmer, G. 1988. 'Seasonal forecasting of the Kenya Coast short rains', *Int. J. Climatol.*, **8**, 489–497.

Glantz, M. 1974. 'Floods, fires, and famines. It is El-Niño to blame', *Oceanus*, **27**, 14–19.
Halpert, M.S. and Ropelewski, C.F. 1992. 'Surface temperature patterns associated with the Southern Oscillation', *J. Climate*, **5**, 577–593.
Indeje, M. and Anyamba, E.K. 1998. 'Sensitivity of mesoscale systems over Kenya to changes in roughness length', *J. African Meteorol. Soc.*, **3**, 19–33.
Janowiak, J. 1988. 'An investigation of Interannual rainfall', *J. Climate*, **1**, 240–255.
Kraiser, H.F. 1959. 'Computer program for varimax rotation in factor analysis', *Educ. Psychol. Meas.*, **19**, 413–420
Kutzbach, J.E. 1967. 'Empirical eigenvectors of sea level pressure, surface temperature and precipitation complexes over north America', *J. Appl. Meteorol.*, **6**, 791–802.
Mukabana, J.R. and Pielke, R.A. 1996. 'Investigating the influence of synoptic-scale monsoonal winds and mesoscale circulations and diurnal weather patterns over Kenya using a mesoscale numerical model', *Mon. Weather Rev.*, **124**, 224–243.
Mutai, C.C., Ward, M.N. and Coleman, A.W. 1998. 'Towards the prediction of the East Africa short rains based on sea-surface temperature–atmosphere coupling', *Int. J. Climatol.*, **18**, 975–997.
Nicholson, S.E. 1996. *The Limnology, Climatology and Paleoclimatology of the East African Lakes*. Gordon and Breach, New York, 57 pp.
Nicholson, S.E. and Nyenzi, B.S. 1990. 'Temporal and spatial variability of SSTs in the tropical Atlantic and Indian Oceans', *Meteorol. Atmos. Phys.*, **42**, 1–17.
Nicholson, S.E., Kim, J., Hoopingarner, J. 1988. *Atlas of African Rainfall and Its Variability*. Department of Meteorology, Florida State University, Tellahassee, FL, 237 pp.
North, G.R., Bell, T.L. and Cahalan, R.F. 1982. 'Sampling errors in estimation of empirical orthogonal functions', *A. Meteorol. Soc.*, **110**, 699–706.
Nyenzi, B.S. 1990. 'An analysis of interannual variability of rainfall over East Africa', *Proceedings of the Second Technical Conference on Weather Forecasting in the Eastern and Southern Africa*, Nairobi, Kenya, pp. 36–41.
Ogallo, L.J. 1980. 'Rainfall variability in Africa', *Mon. Weather Rev.*, **107**, 1133–1139.
Ogallo, L.J. 1983. 'Quasi-periodic patterns in East African rainfall records', *Kenya J. Sci. Technol.*, **A3**, 43–54.
Ogallo, L.J. 1988. 'Relationships between seasonal rainfall in East Africa and the Southern Oscillation', *J. Climatol.*, **8**, 31–43.
Ogallo, L.J. 1989. 'The spatial and temporal patterns of the East African seasonal rainfall derived from principal component analysis', *Int. J. Climatol.*, **9**, 145–167.
Ogallo, L.J., Okoola, R.E. and Wanjohi, D.N. 1994. 'Characteristics of Quasi-Biennial Oscillation over Kenya and their predictability potential for seasonal rainfall', *Mausam*, **45**(1), 57–62.
Okeyo, A.E. 1986. 'The influence of Lake Victoria on the convective systems over the Kenya highlands', *Proceedings of an International Conference on Short, Medium Range Weather Forecasting*, August, 1986, Tokyo, Japan.
Overland, J.E. and Preisendorfer, R.W. 1982. 'A significance test for principal components applied to a cyclone climatology', *Mon. Weather Rev.*, **110**, 1–4.
Phillips, J.G., Cane, M.A. and Rosenzweig, C. 1998. 'ENSO, seasonal rainfall patterns and simulated maize yield variability in Zimbabwe', *Agr. For. Meteorol.*, **90**, 39–50.
Phillips, J.G. and McIntyre, B. 1999. 'ENSO and interannual rainfall variability in Uganda: Implications for agricultural management', *Int. J. Climatol.* (in press).
Rasmusson, E.M. and Carpenter, R.D. 1983. 'Variation in the tropical sea surface temperatures and sea wind fields associated with the Southern Oscillation/El-Niño', *Mon. Weather Rev.*, **110**, 354–384.
Reverdin, G., Cadet, D.L. and Gutzler, D. 1986. 'Interannual displacements of convection and surface circulation over the equatorial Indian Ocean', *Q. J. R. Meteorol. Soc.*, **112**, 46–67.
Richman, M.D. 1981. 'Obliquely rotated principal components. An improved meteorological map typing technique', *J. Appl. Meteorol.*, **20**, 1145–1159.
Rodhe, H. and Virji, H. 1976. 'Trends and periodicities in East Africa rainfall data', *Mon. Weather Rev.*, **104**, 307–315.
Ropelewski, C.F. and Halpert, M.S. 1987. 'Global and regional scale precipitation patterns associated with the El-Niño/Southern Oscillation', *Mon. Weather Rev.*, **115**, 1606–1626.
Semazzi, F.H.M., Burns, B., Lin, N.H. and Schemm, J.K. 1996. 'A GCM study of the teleconnections between the continental climate of Africa and global sea-surface temperature anomalies', *J. Climate*, **9**, 2480–2497.
Semazzi, F.H.M. and Indeje, M. 1999. 'Inter-seasonal variability of ENSO rainfall signal over Africa', *J. African Meteorol. Soc.* (in press).
Sun, L., Semazzi, F.H.M., Giorgi, F. and Ogallo, L.J. 1999a. 'Application of the NCAR regional climate model to Eastern Africa. Part I: simulations of autumn rains of 1988', *J. Geophys. Res.*, **104**(D6), 6529–6548.
Sun, L., Semazzi, F.H.M., Giorgi, F., and Ogallo, L.J. 1999b. 'Application of the NCAR regional climate model to Eastern Africa. Part II: simulations of interannual variability', *J. Geophy. Res.*, **104**(D6), 6549–6562.
Tremberth, K.E. 1974. 'A quasi-biennial standing wave in the southern hemisphere and interrelations with sea surface temperature', *Q. J. R. Meteorol. Soc.*, **101**, 55–74.
Trenberth, K.E. 1997. 'The definition of El Nino', *Bull. Am. Meteorol. Soc.*, **78**, 2771–2777.
Vincent, C.E., Davies, T.D. and Beresford, A.K.C. 1979. 'Recent changes in the level of Lake Naivasha, Kenya, as an indicator of equatorial westerlies over East Africa', *Climatic Chance*, **2**, 175–189.
Wagner, R.G. and da Silva, A.M. 1994. 'Surface conditions associated with the anomalous rainfall in the Guinea coastal region', *Int. J. Climatol.*, **14**, 179–199.
Wang, S. 1984. 'The El-Niño events in 1860–1979', *Kexue Tongbao*, **30**, 728–932.
Weare, B.C., Navato, A.R. and Newell, R.E., 1975. 'Empirical orthogonal analysis of Pacific seas surface temperatures', *Proceedings of the WMO/IAMAP Symposium on Long-term Climatic Fluctuations*, Norwich, England, pp. 167–174.

